AFGL-TR-77-0005
AIR FORCE SURVEYS IN GEOPHYSICS, NO. 358

Atlas of Cloud-Free Line-of-Sight Probabilities

Part 2: Union of Soviet Socialist Republics

IVER A. LUND
DONALD D. GRANTHAM
CLARENCE B. ELAM, Jr.

30 December 1976

METEOROLOGY DIVISION PROJECT 8624
AIR FORCE GEOPHYSICS LABORATORY
HANSCOM AFB, MASSACHUSETTS 01731

AIR FORCE SYSTEMS COMMAND, USAF

Unclassified

SECURITY CLASSIFICATION OF THIS PAGE (When Data Entered)

REPORT DOCUMENTATION PAGE		READ INSTRUCTIONS BEFORE COMPLETING FORM
1. REPORT NUMBER AFGL-TR-77-0005	2. GOVT ACCESSION NO.	3. RECIPIENT'S CATALOG NUMBER
4. TITLE (and Subtitle) ATLAS OF CLOUD-FREE LINE-OF-SIGHT PROBABILITIES, PART 2: Union of Soviet Socialist Republics		5. TYPE OF REPORT & PERIOD COVERED Scientific. Interim. 6. PERFORMING ORG. REPORT NUMBER AFSG No. 358
7. AUTHOR(s) Iver A. Lund Donald D. Grantham Clarence B. Elam, Jr.*		8. CONTRACT OR GRANT NUMBER(s)
9. PERFORMING ORGANIZATION NAME AND ADDRESS Air Force Geophysics Laboratory (LY) Hanscom AFB, Massachusetts 01731		10. PROGRAM ELEMENT, PROJECT, TASK AREA & WORK UNIT NUMBERS 62101F 86240102
11. CONTROLLING OFFICE NAME AND ADDRESS Air Force Geophysics Laboratory (LY) Hanscom AFB, Massachusetts 01731		12. REPORT DATE 30 December 1976 13. NUMBER OF PAGES 83
14. MONITORING AGENCY NAME & ADDRESS(if different from Controlling Office)		15. SECURITY CLASS. (of this report) Unclassified 15a. DECLASSIFICATION/DOWNGRADING SCHEDULE

16. DISTRIBUTION STATEMENT (of this Report)

Approved for public release; distribution unlimited.

17. DISTRIBUTION STATEMENT (of the abstract entered in Block 20, if different from Report)

18. SUPPLEMENTARY NOTES

*USAF Environmental Technical Applications Center, Scott AFB, Illinois 62225

19. KEY WORDS (Continue on reverse side if necessary and identify by block number)

Clouds
Line-of-sight
Climatology
Seeing
Sky cover

20. ABSTRACT (Continue on reverse side if necessary and identify by block number)

This is the second part of a planned Northern Hemisphere atlas of probabilities of cloud-free lines-of-sight between the earth and space. The probabilities are for the mid-season months—January, April, July, and October; four times of the day—0000-0200 LST, 0600-0800 LST, 1200-1400 LST, and 1800-2000 LST; and three elevation angles—10°, 30°, and 90°.

DD FORM 1 JAN 73 1473 EDITION OF 1 NOV 65 IS OBSOLETE

Unclassified

SECURITY CLASSIFICATION OF THIS PAGE (When Data Entered)

Contents

Illustrations

Tables

Atlas of Cloud-Free Line-of-Sight Probabilities Part 2: Union of Soviet Socialist Republics

I. INTRODUCTION

The increased use of optical, infrared, and microwave observing and transmitting devices has resulted in a greater demand for information on humidity, haze, clouds, and precipitation. The Air Force Geophysics Laboratory (AFGL)* Climatology and Dynamics Branch (LYD), L. G. Hanscom AFB, MA 01731, and the USAF Environmental Technical Applications Center (ETAC)*, Scott AFB, Illinois 62225, have responded to this demand by collecting special observations, developing models for estimating the desired information in the absence of direct observations, and processing vast quantities of data.

One of the items frequently requested is information on the probability of a cloud-free line-of sight (CFLOS) between a specific point on the surface of the earth and an aircraft or an object in space. A large volume of data has been processed in response to these requests.

(Received for publication 29 December 1976)

*Department of Defense organizations and contractors are encouraged to contact AFGL or ETAC for additional information on line-of-sight probabilities. Persistence, recurrence, joint probabilities, and probabilities as a function of altitude are available.

AFGL and ETAC are endeavoring to prepare a Northern Hemisphere atlas from these data. Because this is a very time-consuming effort, we have decided to prepare the atlas in sections as data become available. The first section depicting CFLOS probabilities over Germany has been published.[1]

2. THE MODEL

Lund and Shanklin[2] developed models for estimating probabilities of CFLOS through the atmosphere at any desired elevation angle and geographical location. The models require a knowledge of sky-cover climatology for the locations.

The model used to estimate CFLOS probabilities through the entire atmosphere can be expressed as follows:

$$ {}_{\alpha}\hat{P}_1 = {}_{\alpha}C_s K_1 \qquad (1) $$

where ${}_{\alpha}\hat{P}_1$ is a column vector of α rows, one row for each angle considered; ${}_{\alpha}C_s$ is a matrix of α rows and s columns, one column for each sky cover category; and ${}_sK_1$ is a column vector of s rows. The $\hat{P}$ values are estimates of CFLOS probabilities, the C values are CFLOS probabilities at angles α given k octas of cloudiness, and the K values are probabilities of each k octa of cloudiness.

The ${}_{\alpha}C_s$ matrix used for this paper is given in Table 1.

Table 1. Probabilities of Cloud-Free Lines-of-Sight as a Function of Elevation Angle and Observed Total Sky Cover, in Octas. This is the ${}_{\alpha}C_s$ Matrix

Elevation Angle (Degrees)	Sky Cover (octas)								
	0	1	2	3	4	5	6	7	8
90	1.00	0.96	0.89	0.83	0.77	0.68	0.55	0.35	0.08
30	0.98	0.92	0.83	0.75	0.66	0.55	0.43	0.28	0.06
10	0.97	0.84	0.72	0.58	0.47	0.38	0.28	0.17	0.03

1. Lund, I.A., Grantham, D.D., and Elam, C.B., Jr. (1975) Atlas of Cloud-Free Line-of-Sight Probabilities, Part 1: Germany, AF Surveys in Geophysics No. 309, AFCRL-TR-75-0281, 77 pp.

2. Lund, I.A. and Shanklin, M.D. (1973) Universal methods for estimating probabilities of cloud-free lines-of-sight through the atmosphere, J. Appl. Meteorol. 12(No. 1):28-35.

3. AN EXAMPLE

The climatic record of sky cover at Moscow, U.S.S.R., shows that 0/8, 1/8, ... 7/8, and 8/8 sky cover was reported 9.9, 1.1, 3.2, 1.6, 2.7, 3.2, 6.5, 16.7, and 55.1 percent of the time, respectively, at 1200 LST for the month of January, 1946 through 1971. Performing the matrix multiplication, we obtain:

$$\alpha\hat{P}_1 = \begin{bmatrix} 1.00 & 0.96 & ..... & 0.35 & 0.08 \\ 0.98 & 0.92 & ..... & 0.28 & 0.06 \\ 0.97 & 0.84 & ..... & 0.17 & 0.03 \end{bmatrix} \begin{bmatrix} 0.099 \\ 0.011 \\ . \\ . \\ 0.167 \\ 0.551 \end{bmatrix} = \begin{bmatrix} 0.332 \\ 0.289 \\ 0.226 \end{bmatrix} \quad (2)$$

The computations show that there is a 33.2 percent probability of a CFLOS at Moscow looking toward the zenith (90°), and a 28.9 percent and 22.6 percent probability of a CFLOS at 30° and 10° elevation angles, respectively.

4. THE STATIONS

Table 2 lists stations from which long records of hourly sky cover observations are available for at least part of the day. CFLOS probabilities were computed for these stations, which are shown in Figure 1.

Table 2. Station Locator Table

Map Number	WMO Number (Call Letters)	Station Name	Lat. (°N)	Long. (°E)	Alt. (m)
1	33393	Lvov	49°49'	23°57'	325
2	33837	Odessa	46°29'	30°38'	64
3	33946	Simferopol	45°02'	33°59'	204
4	34731	Rostov-Na-Donu	47°15'	39°49'	77
5	34122	Voronezh	51°42'	30°10'	164
6	34300	Khar'kov	49°56'	36°17'	152
7	33345	Kiev/Julyany	50°24'	30°27'	179
8	26850	Minsk/Loshita	53°52'	27°32'	234
9	26629	Kuanas	54°53'	23°53'	75
10	26038	Tallin	59°25'	24°48'	44
11	26477	Velikiye Luki	56°23'	30°36'	98
12	27612	Moscow	55°45'	37°34'	161
13	27037	Vologda	59°17'	39°52'	118
14	22837	Vytegra	61°01'	36°27'	59
15	26063	Leningrad	59°58'	30°18'	4

Table 2. Station Locator Table (Cont)

Map Number	WMO Number (Call Letters)	Station Name	Lat. (°N)	Long. (°E)	Alt. (m)
16	22602	Reboly	63°49'	30°49'	181
17	22550	Archangel'sk	64°35'	40°30'	13
18	22113	Murmansk	68°58'	33°03'	46
19	22165	Kanin Nos	68°39'	43°18'	M
20	37549	Tiflis	41°41'	44°57'	490
21	38507	Krashovodsk	40°02'	52°59'	89
22	38880	Asnkhabad	37°58'	58°20'	230
23	38687	Chardzhou	39°05'	63°36'	193
24	38262	Chimbay	42°57'	59°49'	66
25	35925	Pervyy	45°27'	56°07'	82
26	35700	Gur'yev	47°01'	51°51'	M
27	38001	Fort Shevchenko	44°33'	50°15'	20
28	34880	Astrakhan	46°16'	48°02'	18
29	34172	Saratov	51°34'	46°02'	158
30	35121	Orenburg	51°45'	55°06'	109
31	35358	Turgay	49°38'	63°30'	123
32	28952	Kustanay	53°13'	63°37'	171
33	28440	Sverdlovsk	56°48'	60°38'	237
34	28225	Perm'	58°01'	56°18'	161
35	27595	Kazan	55°47'	49°11'	64
36	27196	Kirov	58°39'	49°37'	164
37	23804	Syktyvkar	61°40'	50°51'	98
38	23724	Njaksimvol	62°28'	60°52'	50
39	28275	Tobolsk Arpt	58°09'	68°11'	44
40	23933	Hanty-Mansijsk	60°58'	69°04'	40
41	23849	Surgut	61°15'	73°30'	43
42	23552	Tarko-Sale	64°55'	77°49'	27
43	23330	Salehard	66°32'	66°32'	35
44	23219	Hoseda-Hard	67°05'	59°23'	81
45	23205	Nar'Jan-Mar	67°39'	53°01'	7
46	23146	Mys Kamennyj	68°28'	73°36'	M
47	20674	O. Dikson	73°30'	80°14'	20
48	20046	Krenkelja	80°37'	58°03'	20
49	20069	O. Vize	79°30'	76°59'	18
50	20292	Celjuskin	77°43'	104°17'	13
51	38457	Tashkent	41°16'	69°16'	428
52	36870	Alma-Ata	43°14'	76°56'	847
53	35796	Balkhash	46°54'	75°00'	423
54	35394	Karaganda	49°48'	73°08'	555
55	28698	Omsk	54°56'	73°24'	94
56	36177	Semipalatinsk	50°21'	80°15'	206
57	29838	Barnaul	53°20'	83°42'	196
58	29231	Kolpashevo	58°18'	82°54'	76
59	23472	Turuhansk	65°47'	87°57'	32
60	23884	Podkamennaj Tung.	61°36'	90°00'	60
61	29263	Enisejsk	58°27'	92°09'	78
62	29574	Krasnoyarsk	56°00'	92°53'	194
63	29865	Abakan	53°45'	91°24'	245
64	30710	Irkutsk	52°16'	104°21'	485
65	30309	Bratsk	56°04'	101°50'	326
66	29282	Boguchany	58°25'	97°24'	134
67	24507	Tura	64°10'	100°04'	140
68	24105	Essej	68°28'	102°22'	200

Table 2. Station Locator Table (Cont)

Map Number	WMO Number (Call Letters)	Station Name	Lat. (°N)	Long. (°E)	Alt. (m)
69	20891	Hatanga	71°59'	102°28'	24
70	24125	Olenek	68°30'	112°26'	127
71	24817	Erbogacen	61°16'	108°01'	M
72	30230	Kirensk	57°46'	108°07'	261
73	30636	Barguzin	53°37'	109°38'	486
74	30758	Chita	52°01'	113°20'	685
75	30554	Bogdarin	54°26'	113°35'	917
76	30469	Kalakan	55°07'	116°45'	607
77	30673	Mogocha	53°44'	119°47'	619
78	31004	Aldan	58°37'	125°22'	682
79	24738	Suntar	62°09'	117°36'	124
80	24641	Viljujsk	63°46'	121°37'	107
81	24959	Jakutsk	62'05'	129°45'	103
82	24266	Verhojansk	67°33'	133°23'	137
83	24143	Dzardzan	68°44'	124°00'	47
84	21432	Ostrov Kotel-Nyj	76°00'	137°54'	10
85	21946	Cokurdan	70°37'	147°53'	48
86	21965	O. Cetryeh/Stolbovo	70°38'	162°24'	6
87	25173	M. Smidta	68°55'	179°29'	7
88	25563	Anadyr	64°47'	177°34'	62
89	25248	Ilirnej	67°20'	168°14'	426
90	25325	Ust'-Oloj	66°33'	159°25'	1250
91	25703	Sejmchan	62°55'	152'25'	207
92	31168	Ayan	56°27'	138°09'	9
93	31369	Nikolayevsk-on-Amur	53°09'	140°42'	47
94	31416	Im. Poliny Osipenko	52°25'	136°30'	65
95	31510	Blagoveshchensk	50°16'	127°30'	137
96	31735	Khabarovsk	48°31'	135°10'	72
97	31960	Vladivostok	43°07'	131°54'	138

5. THE ANALYSIS

A total of 51 maps are included in this paper: one station locator map, Figure 1; one map for each of the four mid-season months (January, April, July, October) covering four 3-hour periods (0000—0200 LST, 0600—0800 LST, 1200—1400 LST, 1800—2000 LST), and three elevation angles (10°, 30°, 90°), Figures 2 through 49; and two maps depicting the extreme conditions (that is, the highest and the lowest probability for any of the above months and periods), Figures 50 and 51. In order to conserve space, the extreme condition is shown only for the 30° elevation angle only.

Eq. (1) was used to compute CFLOS probability values. The ${}_{s}K_{1}$ column vector was changed with every station, month, or 3-hour time period. For the majority of U.S.S.R. stations, the probabilities were based on more than 300 sky-cover observations (that is, at least a 10-year period-of-record). Those probabilities based on less than 300 observations were checked for consistency with surrounding locations

and for diurnal consistency. The probability values were plotted on maps and analyzed as shown in Figures 2 through 51. Because the isolines were drawn strictly to the data, the analysis seldom departs more than 1 or 2 percent from the computed probabilities. Terrain features were not specifically used in the analysis but their effects are obvious, as seen along the Ural Mountains (about 60°E longitude) and in the desert areas north of Iran and Afghanistan.

The CFLOS atlas for Germany, Part 1 of this series, included probabilities for the 50° elevation angle. However, 50° elevation angle probabilities are not included here because an examination of the U.S.S.R. probabilities for 50° elevation angles showed them to be almost always 1 or 2 percent less than CFLOS probabilities for the 90° elevation angles, and they were never more than 2.5 percent less. Probabilities for the 50° elevation angle should be estimated by subtracting 2 percent from the 90° probabilities.

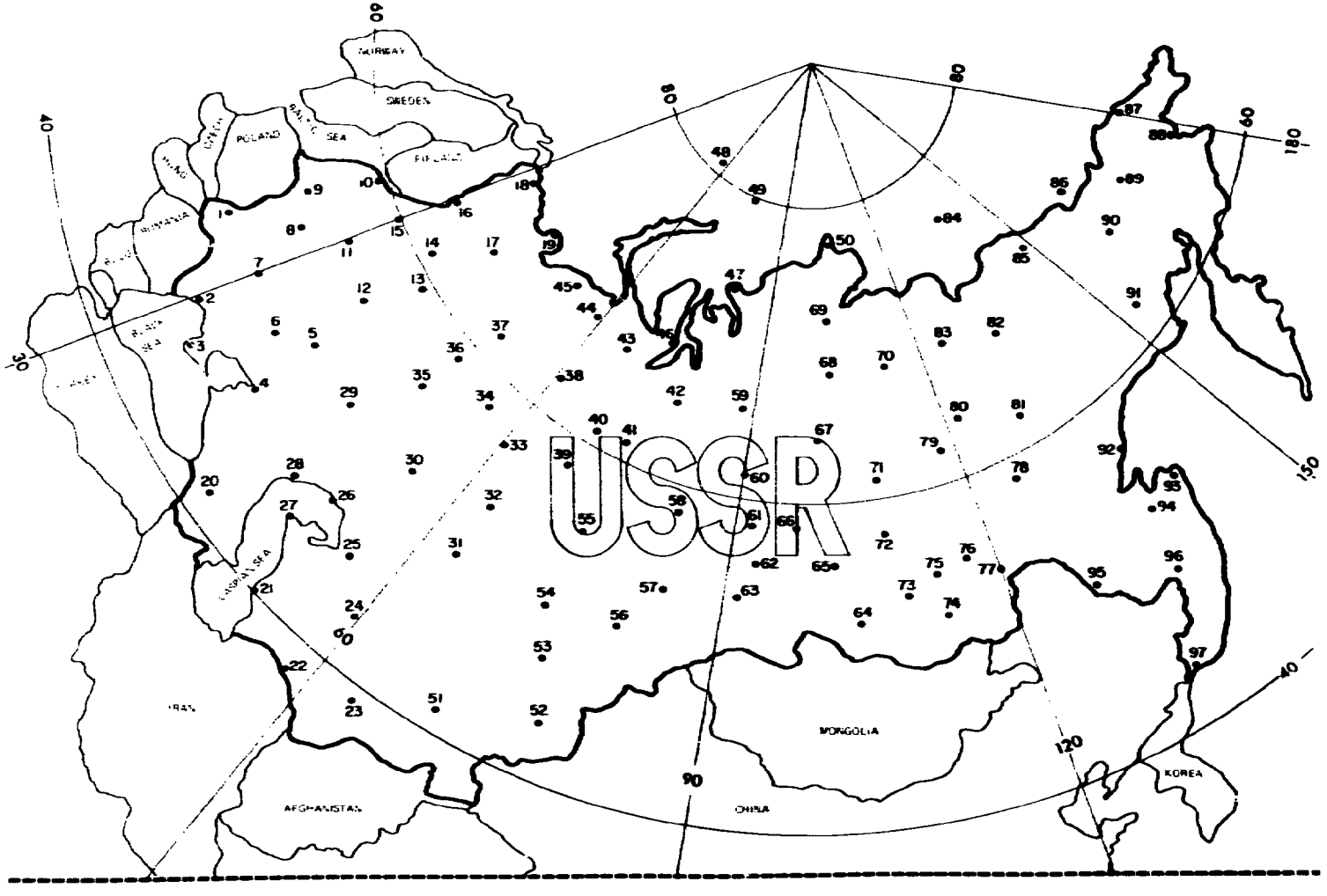

Figure 1. Station Location Map

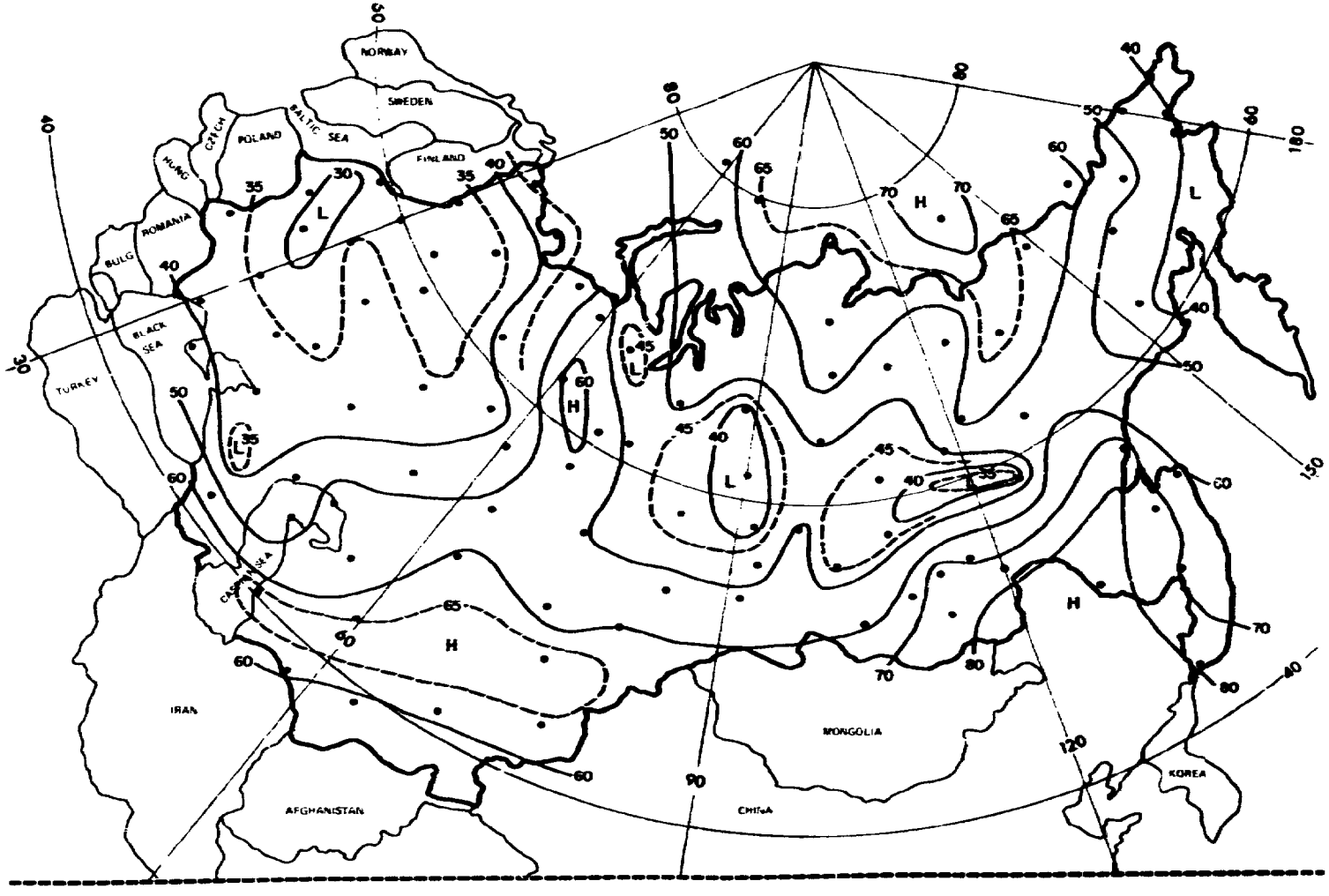

Figure 2. CFLOS Probabilities for Jan, 0000—0200 LST, 90° Elevation

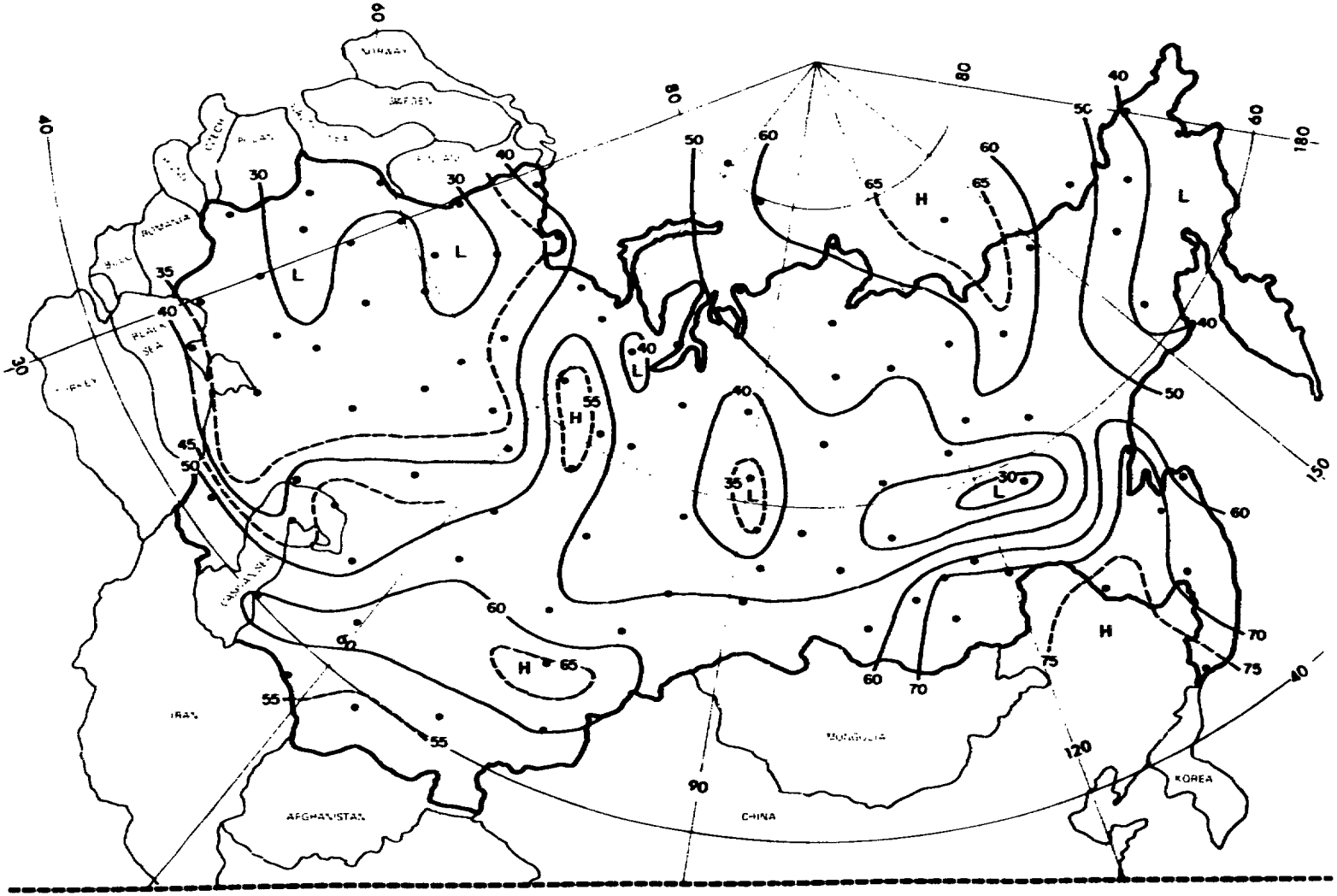

Figure 3. CFLOS Probabilities for Jan, 0000—0200 LST, 30° Elevation

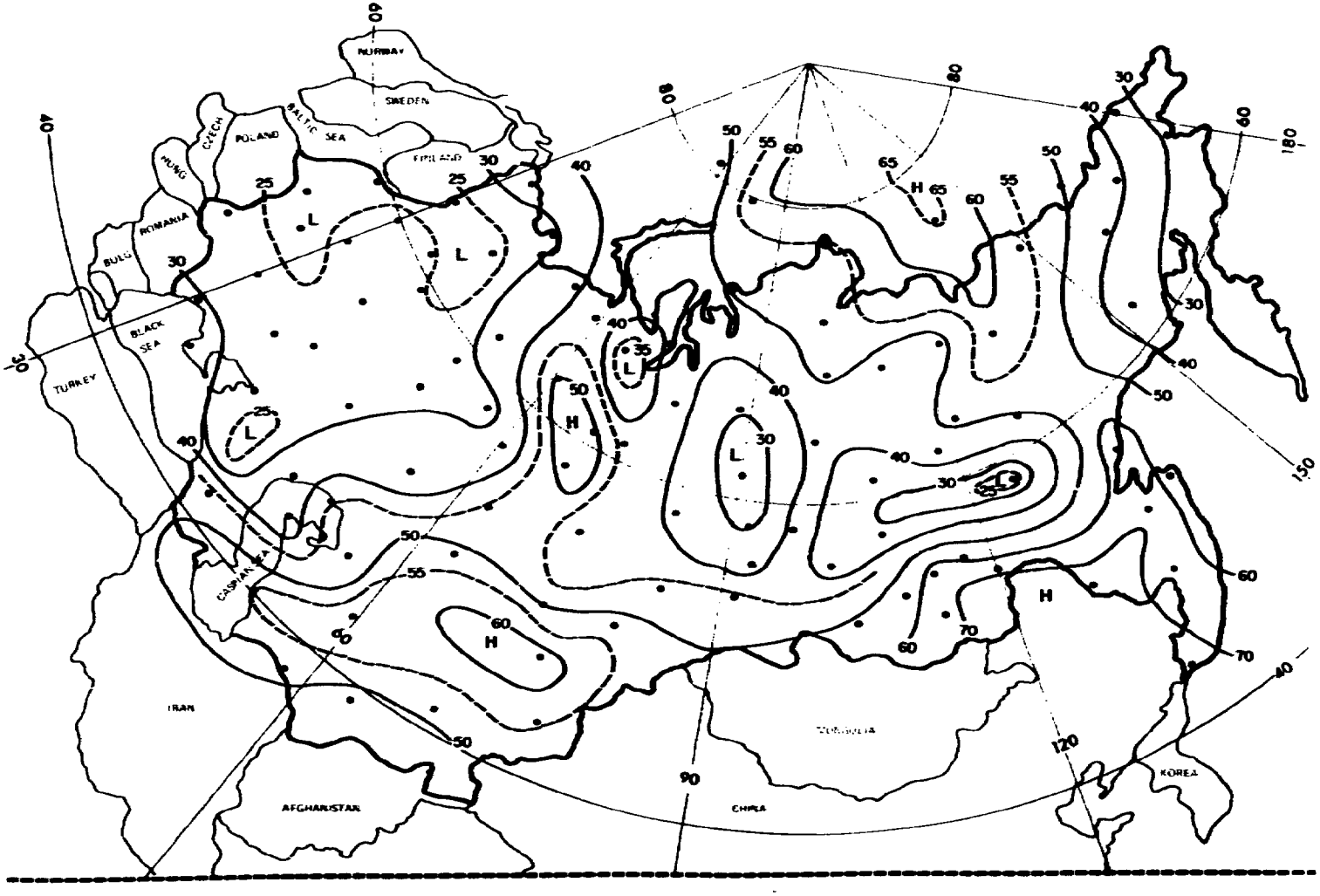

Figure 4. CFLOS Probabilities for Jan, 0000—0200 LST, 10° Elevation

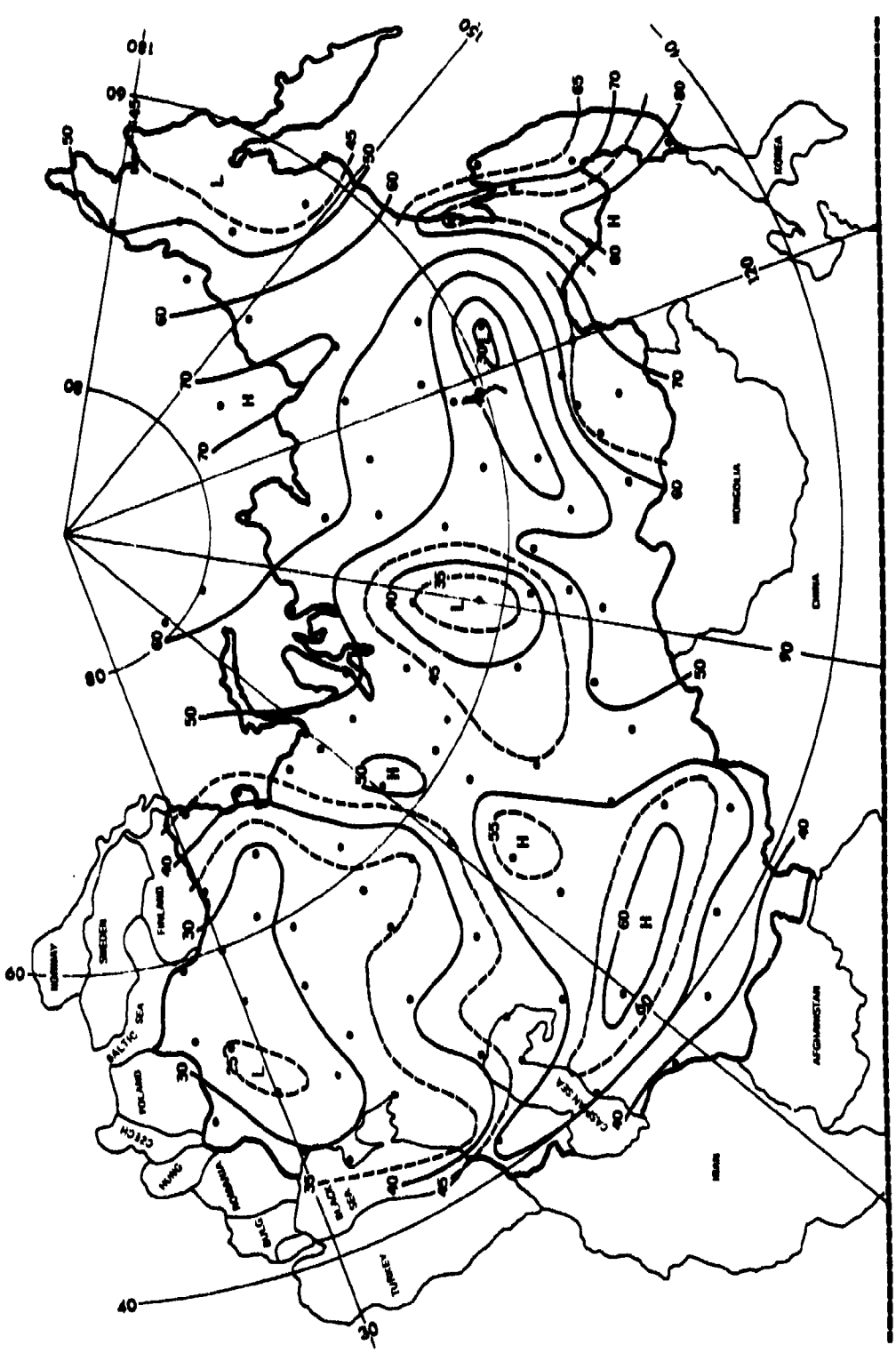

Figure 5. CFLOS Probabilities for Jan, 0600—0800 LST, 90° Elevation

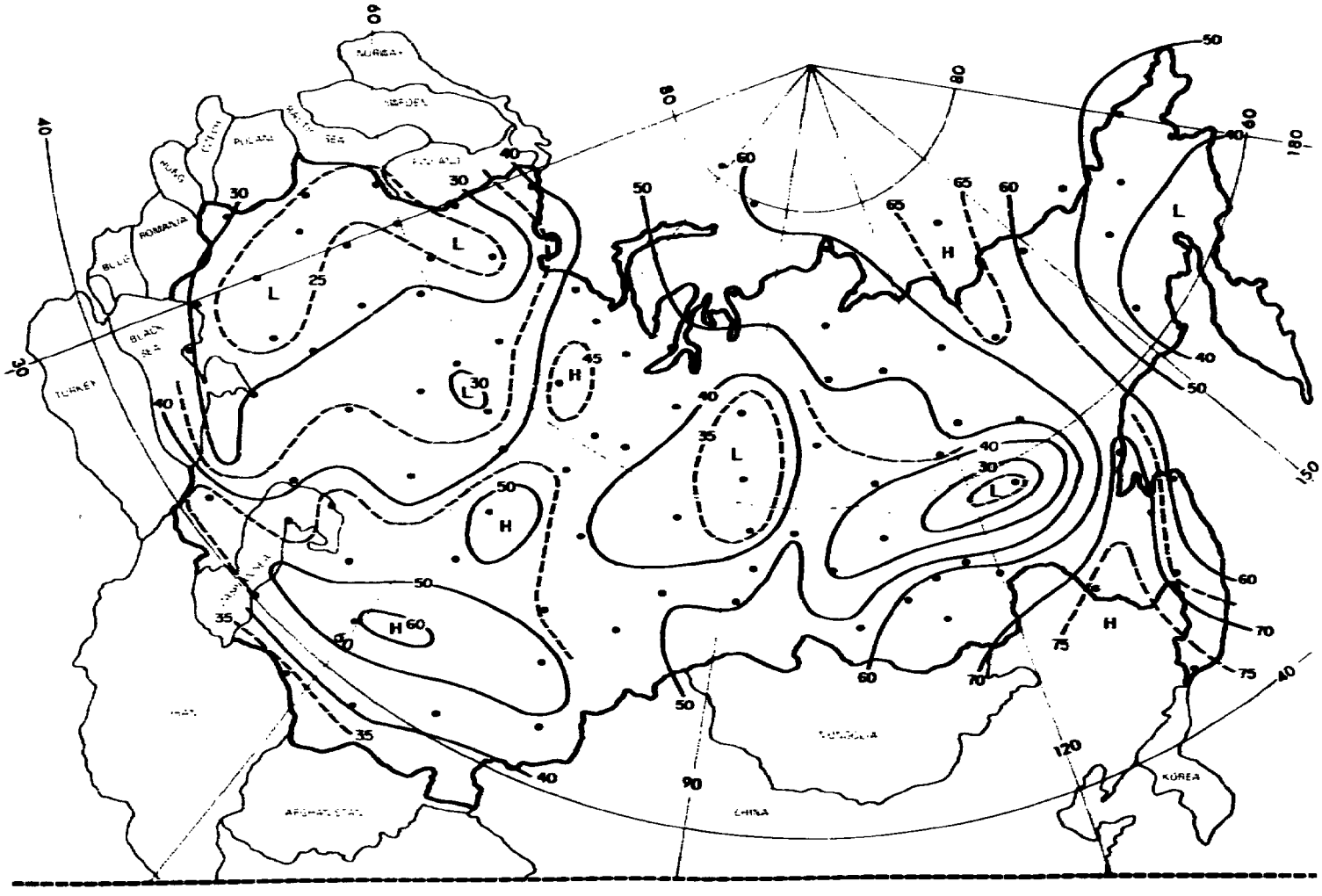

Figure 6. CFLOS Probabilities for Jan, 0600—0800 LST, 30° Elevation

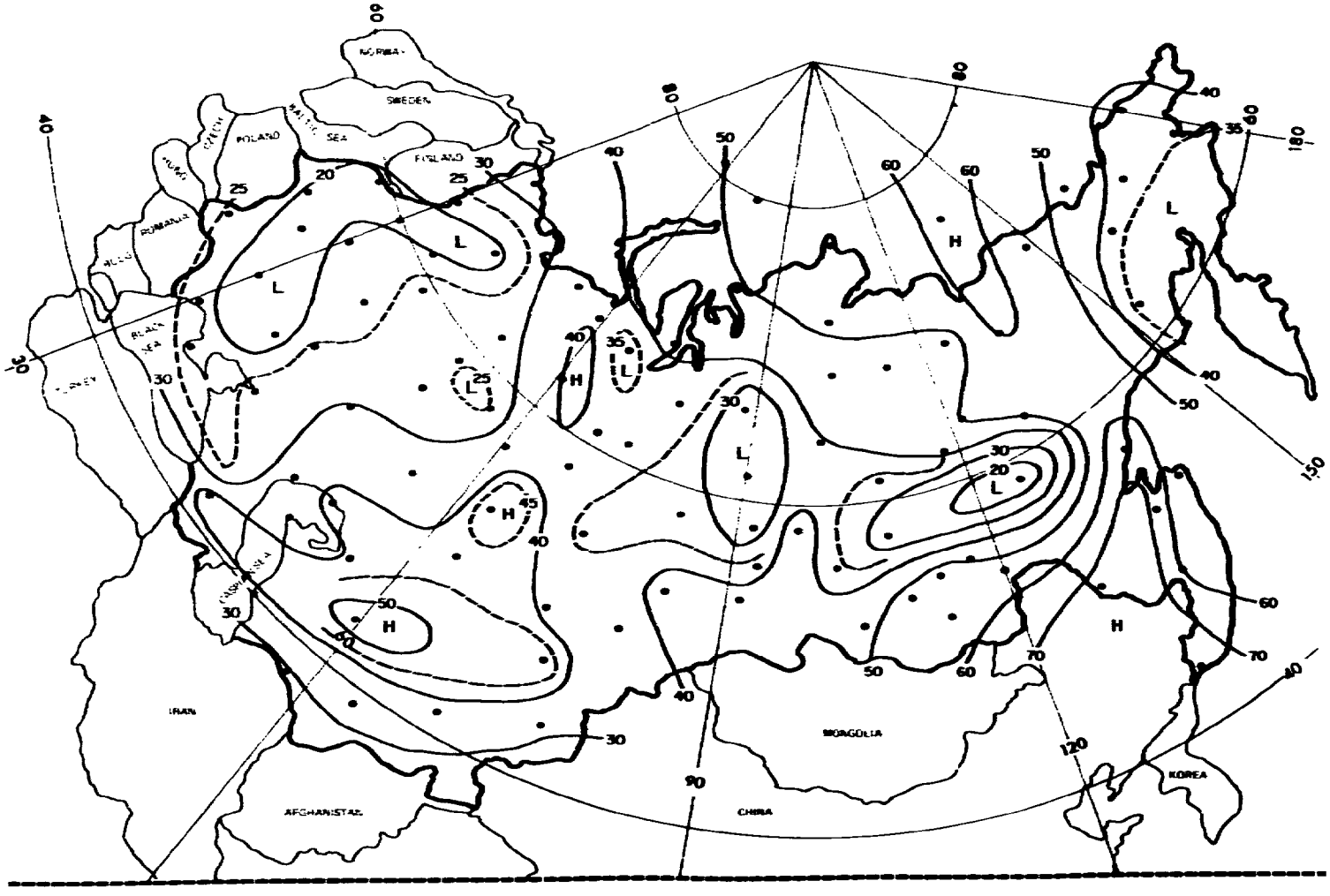

Figure 7, CFLOS Probabilities for Jan, 0600—0800 LST, 10° Elevation

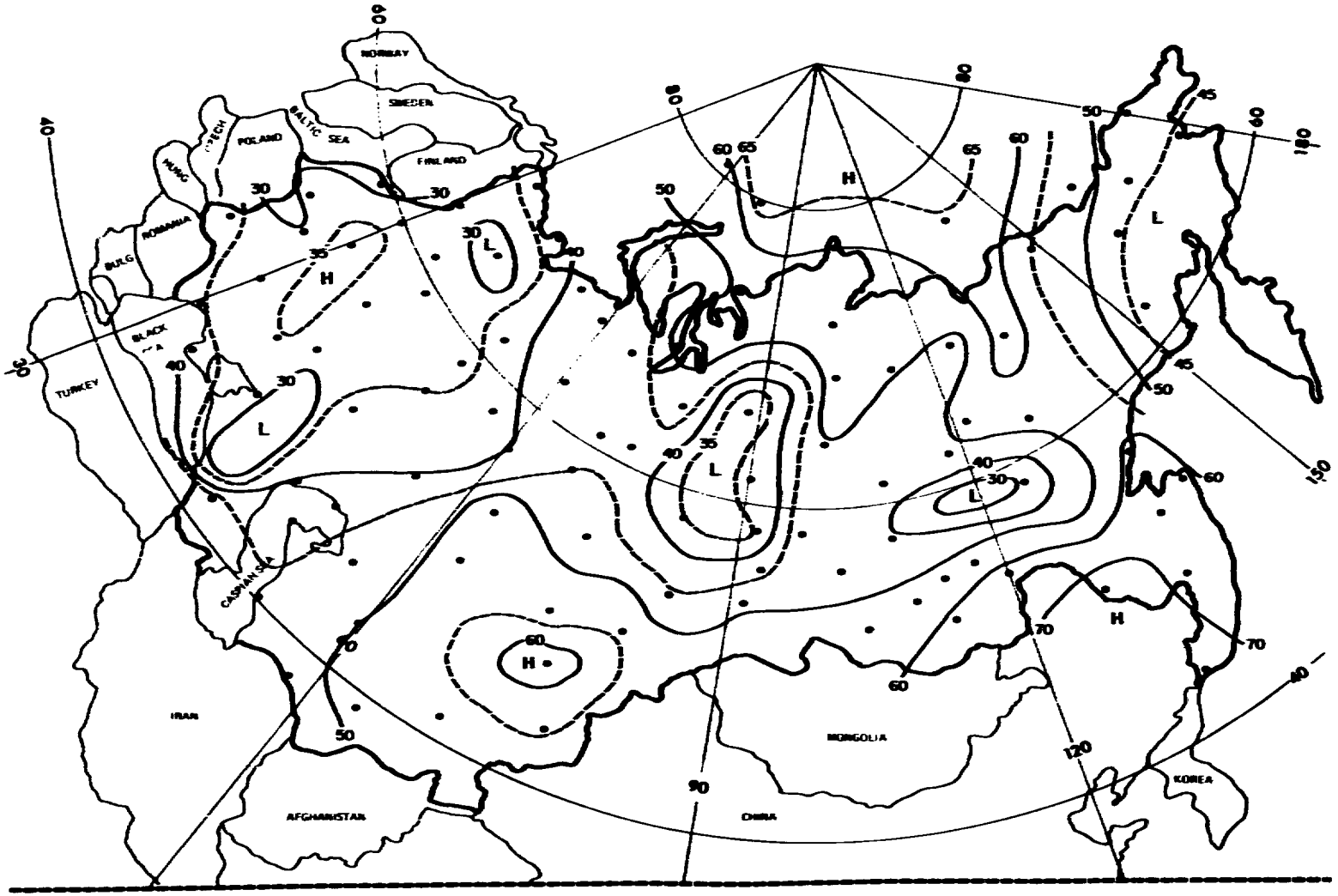

Figure 8. CFLOS Probabilities for Jan, 1200—1400 LST, 90° Elevation

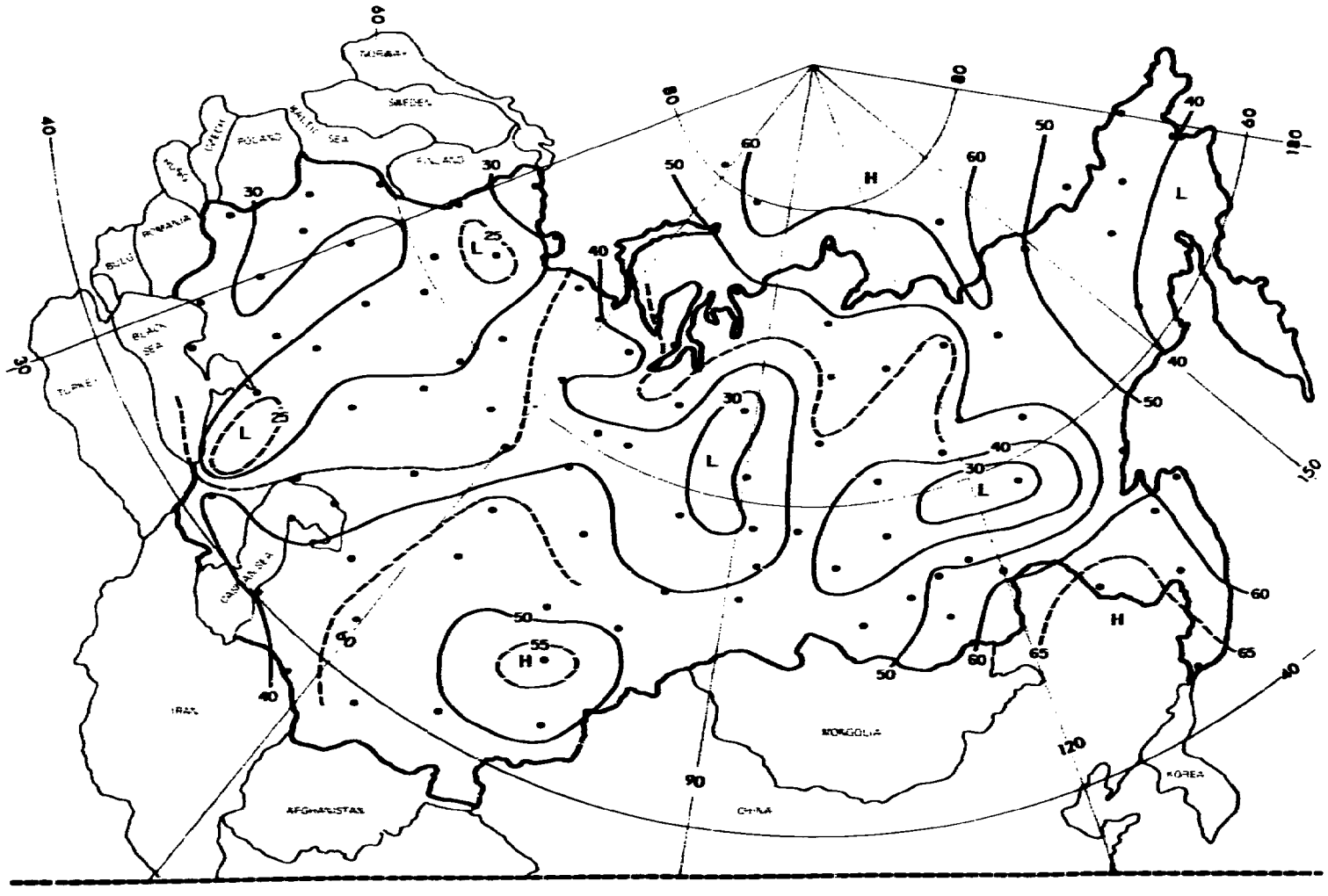

Figure 9. CFLOS Probabilities for Jan, 1200–1400 LST, 30° Elevation

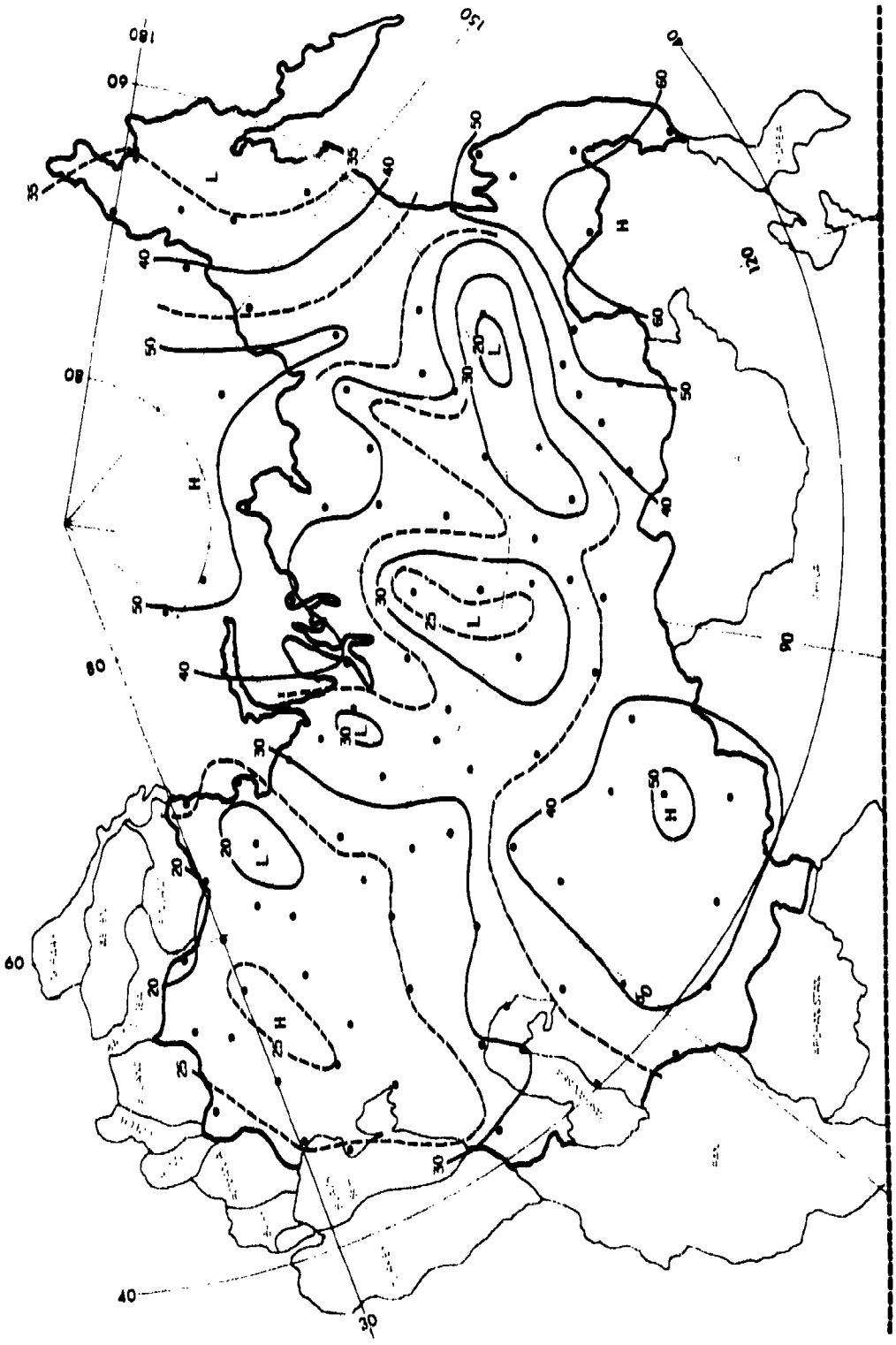

Figure 10. CFLOS Probabilities for Jan, 1200–1400 LST, 10° Elevation

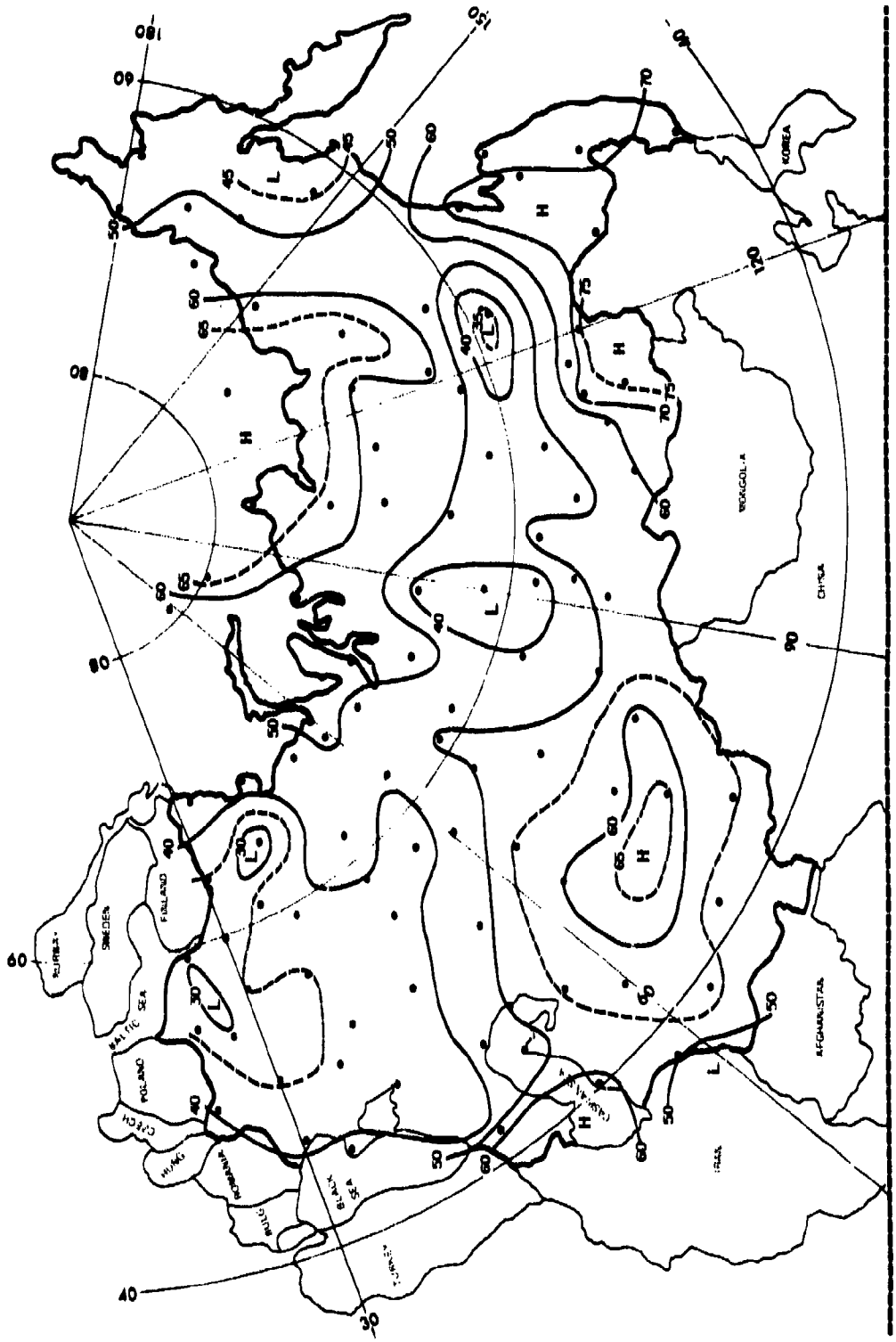

Figure 11. CFLOS Probabilities for Jan, 1800–2000 LST, 90° Elevation

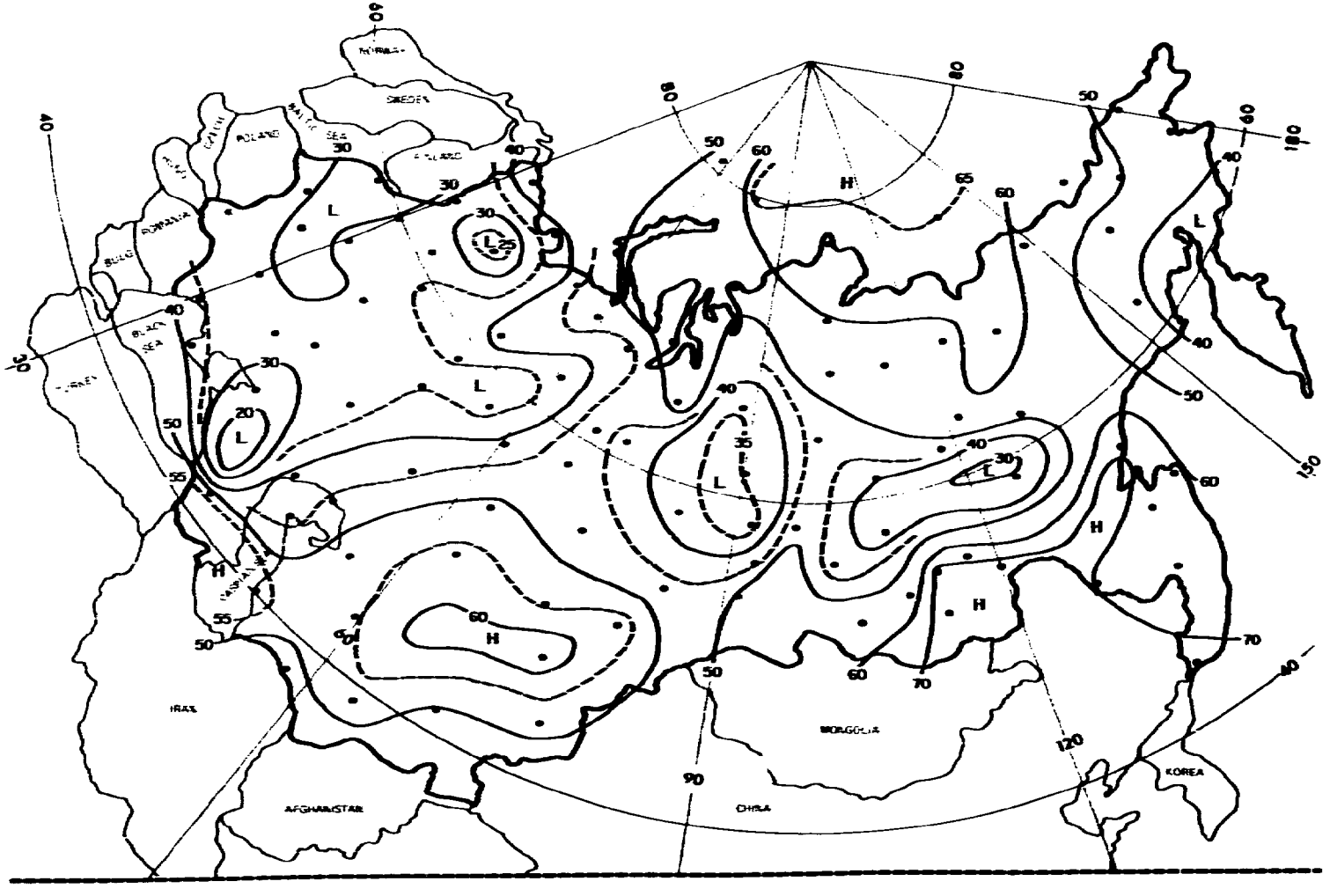

Figure 12. CFLOS Probabilities for Jan, 1800—2000 LST, 30° Elevation

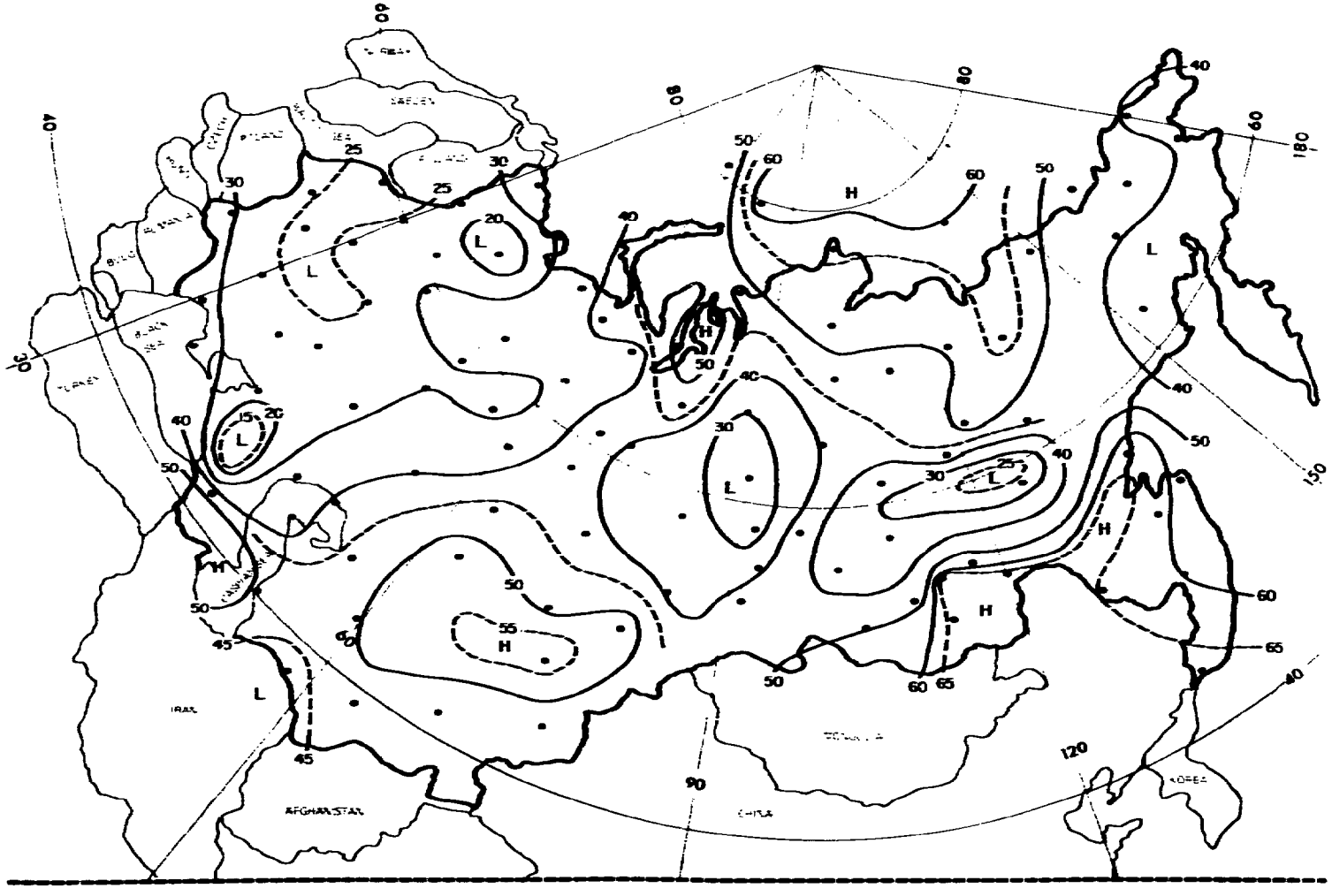

Figure 13. CFLOS Probabilities for Jan, 1800—2000 LST, 10° Elevation

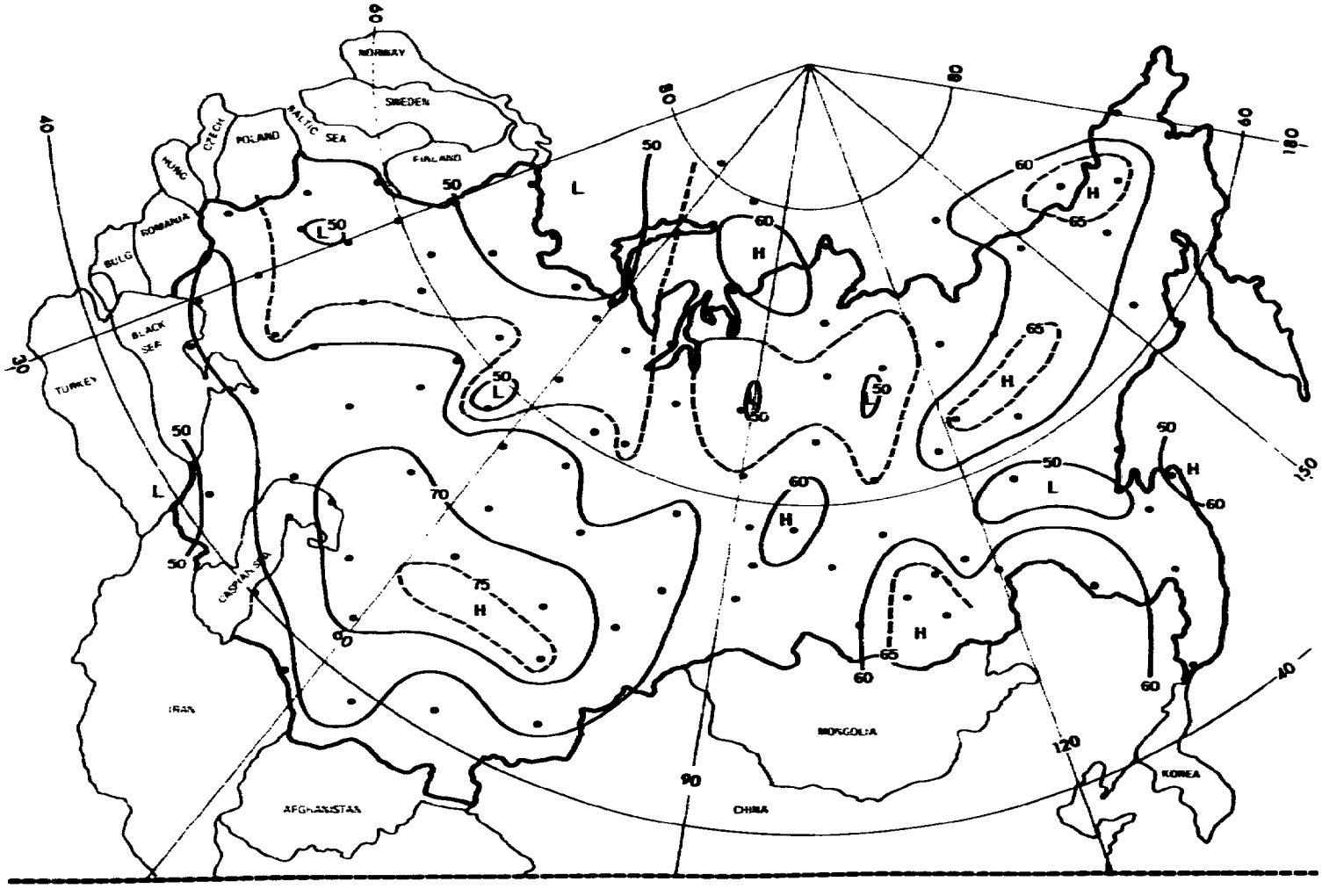

Figure 14. CFLOS Probabilities for Apr, 0000—0200 LST, 90° Elevation

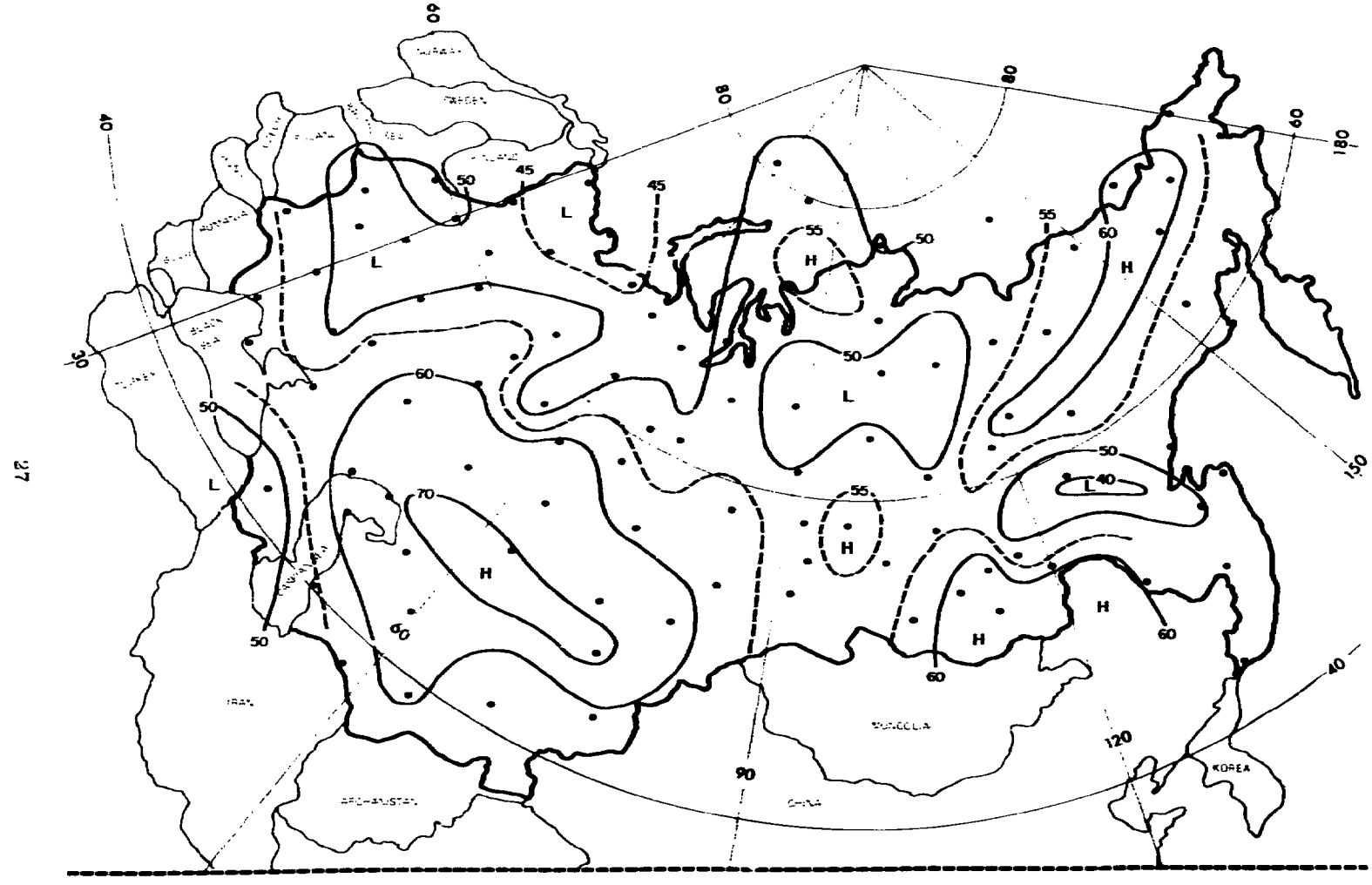

Figure 15. CFLOS Probabilities for Apr, 0000—0200 LST, 30° Elevation

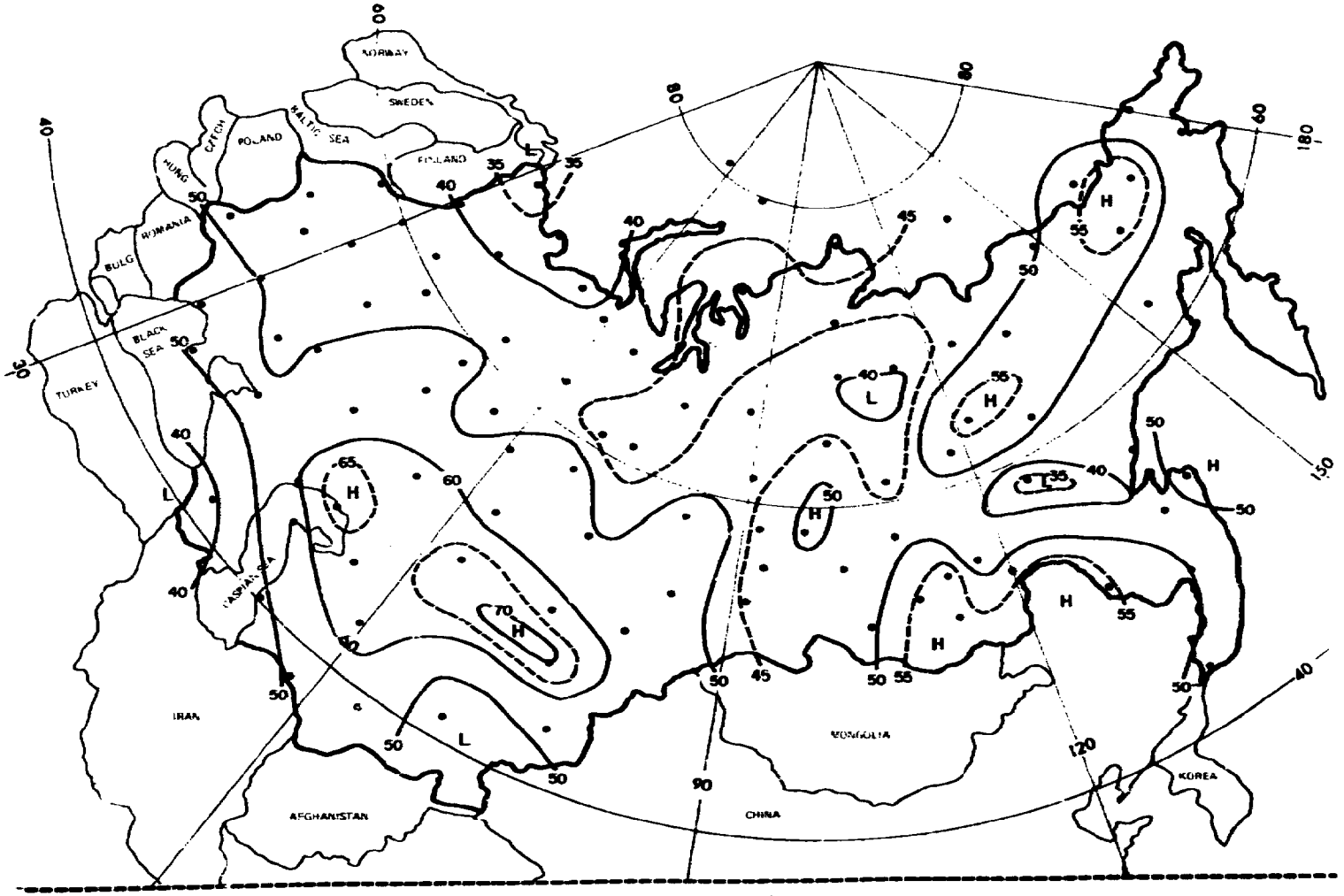

Figure 16. CFLOS Probabilities for Apr, 0000—0200 LST, 10° Elevation

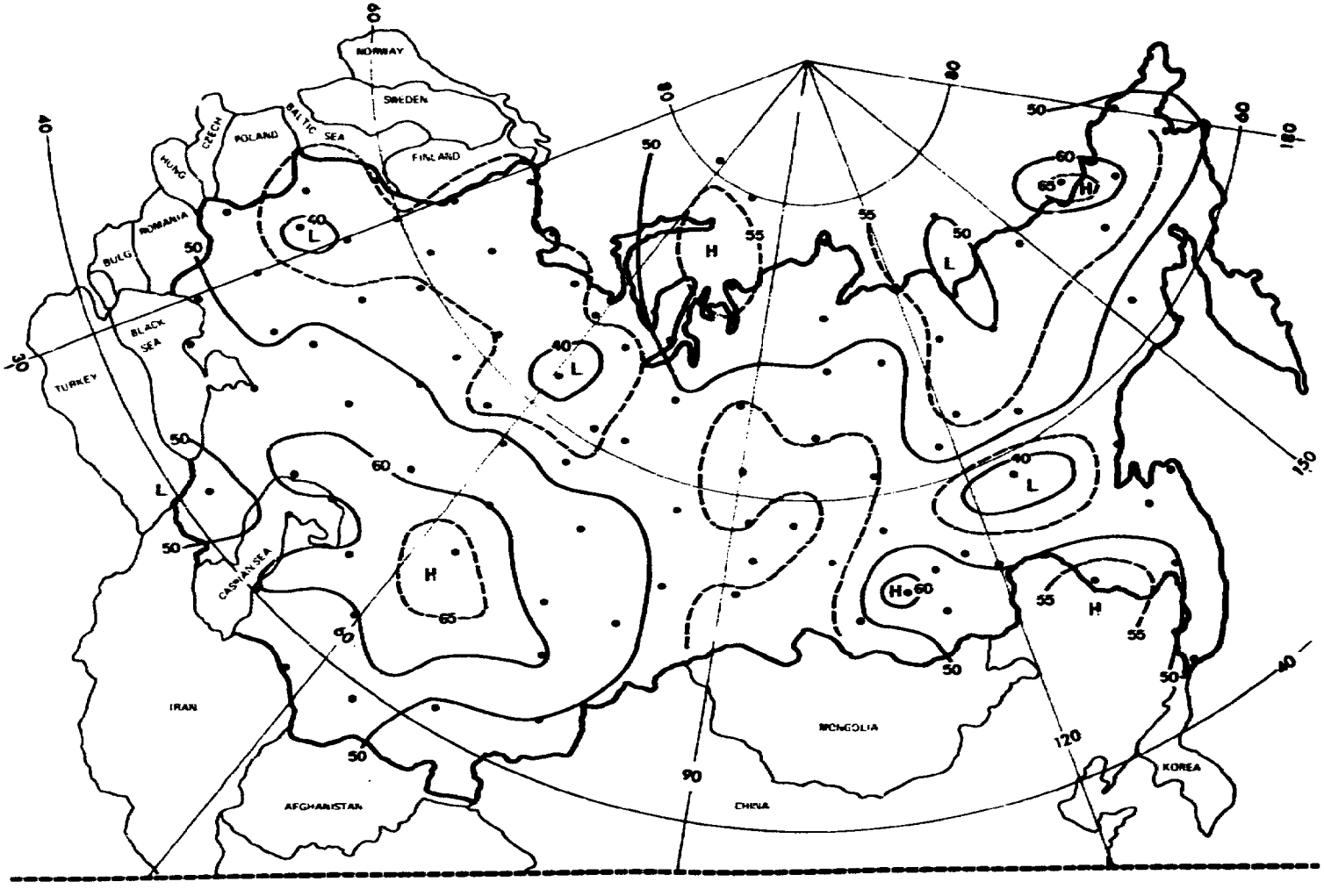

Figure 17. CFLOS Probabilities for Apr, 0600—0800 LST, 90° Elevation

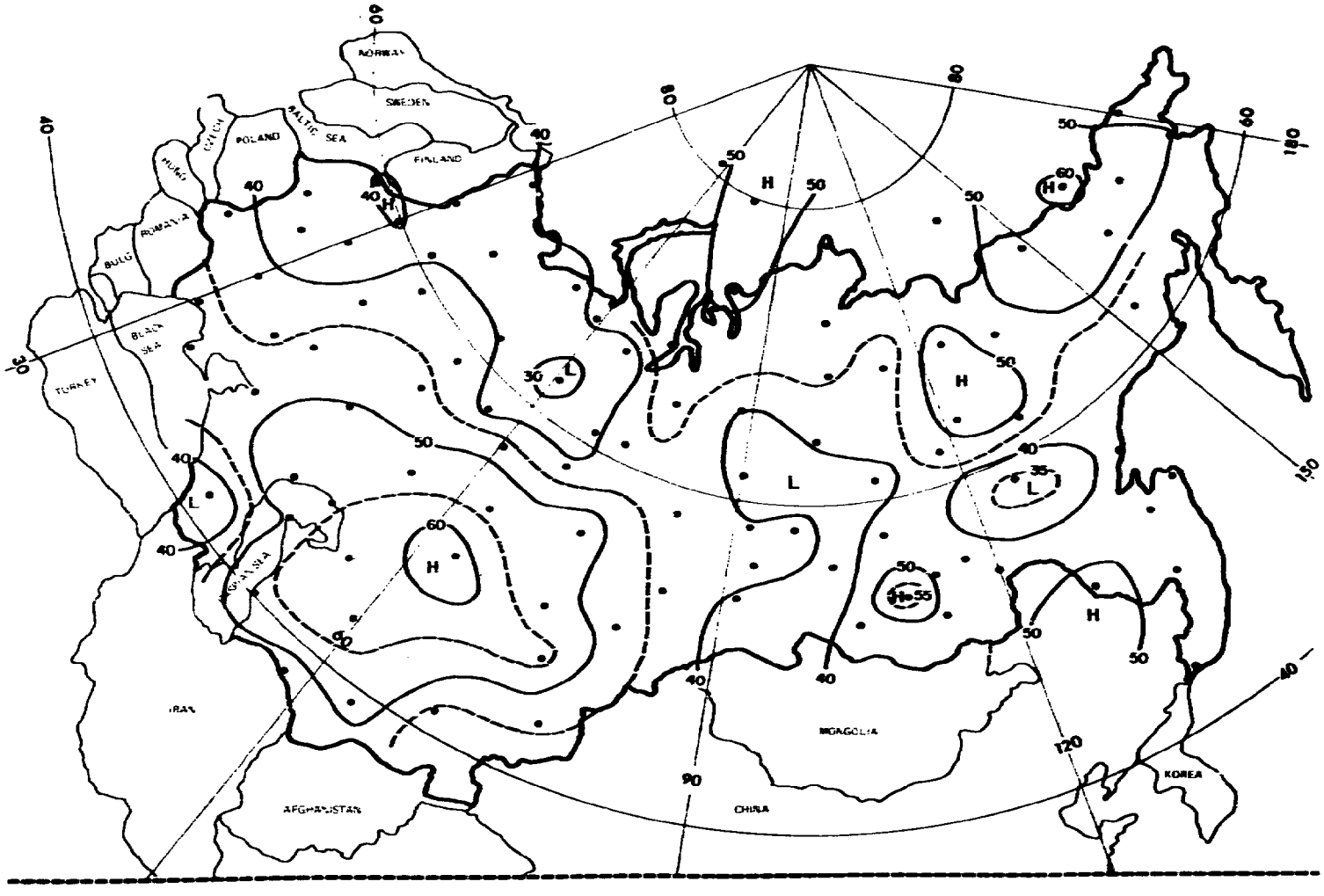

Figure 18. CFLOS Probabilities for Apr, 0600—0800 LST, 30° Elevation

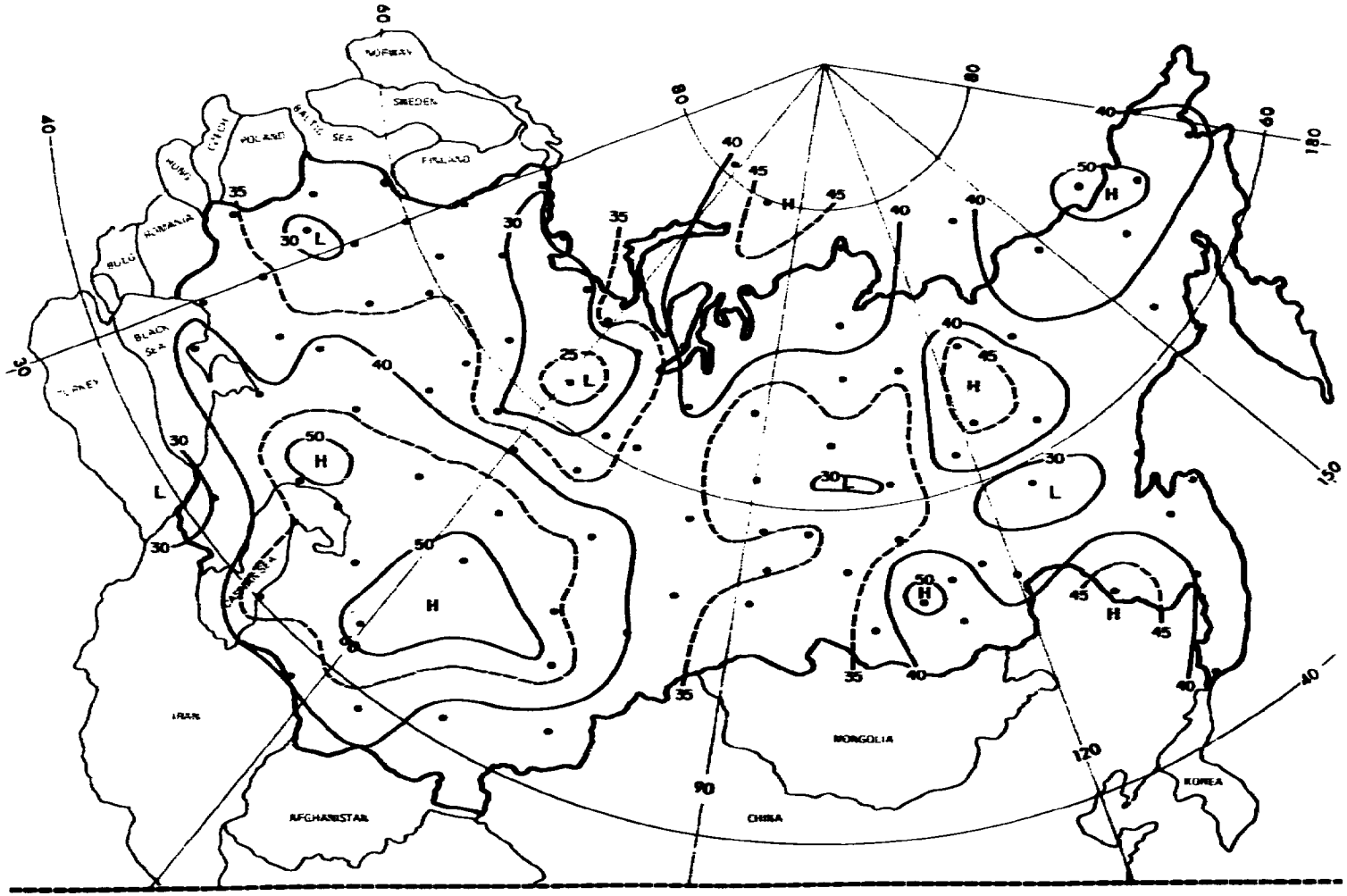

Figure 19. CFLOS Probabilities for Apr, 0600—0800 LST, 10° Elevation

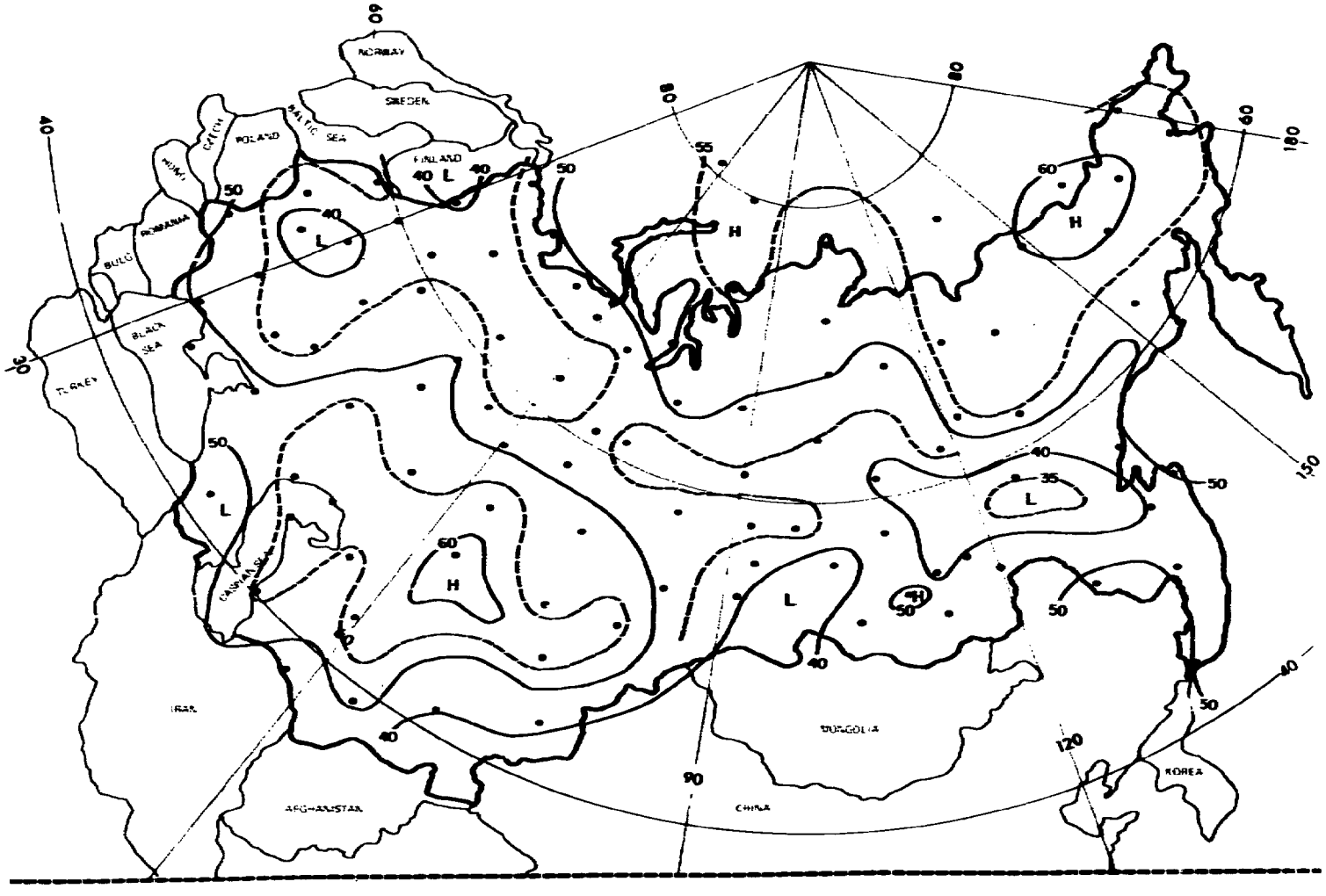

Figure 20. CFLOS Probabilities for Apr, 1200—1400 LST, 90° Elevation

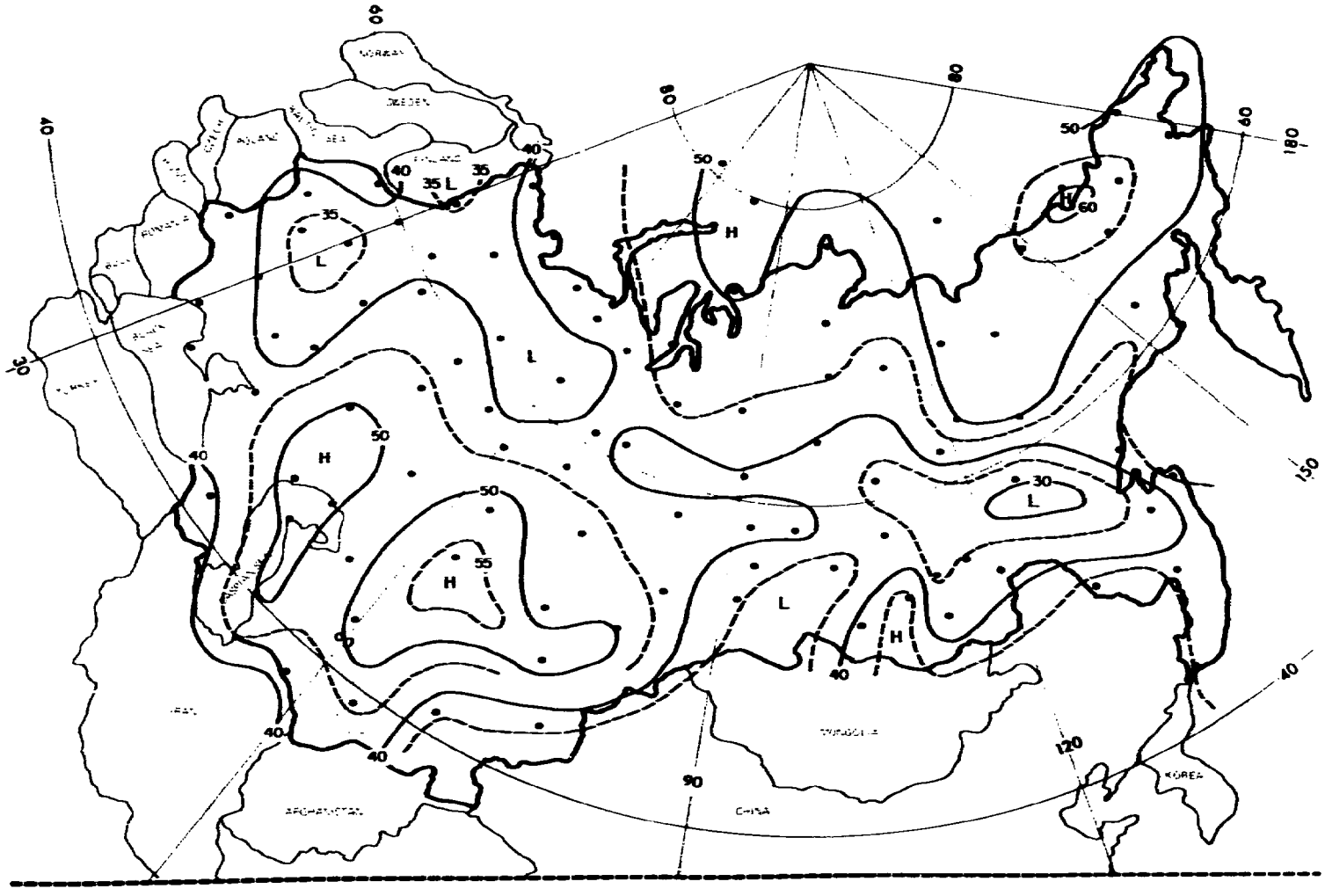

Figure 21. CFLOS Probabilities for Apr, 1200—1400 LST, 30° Elevation

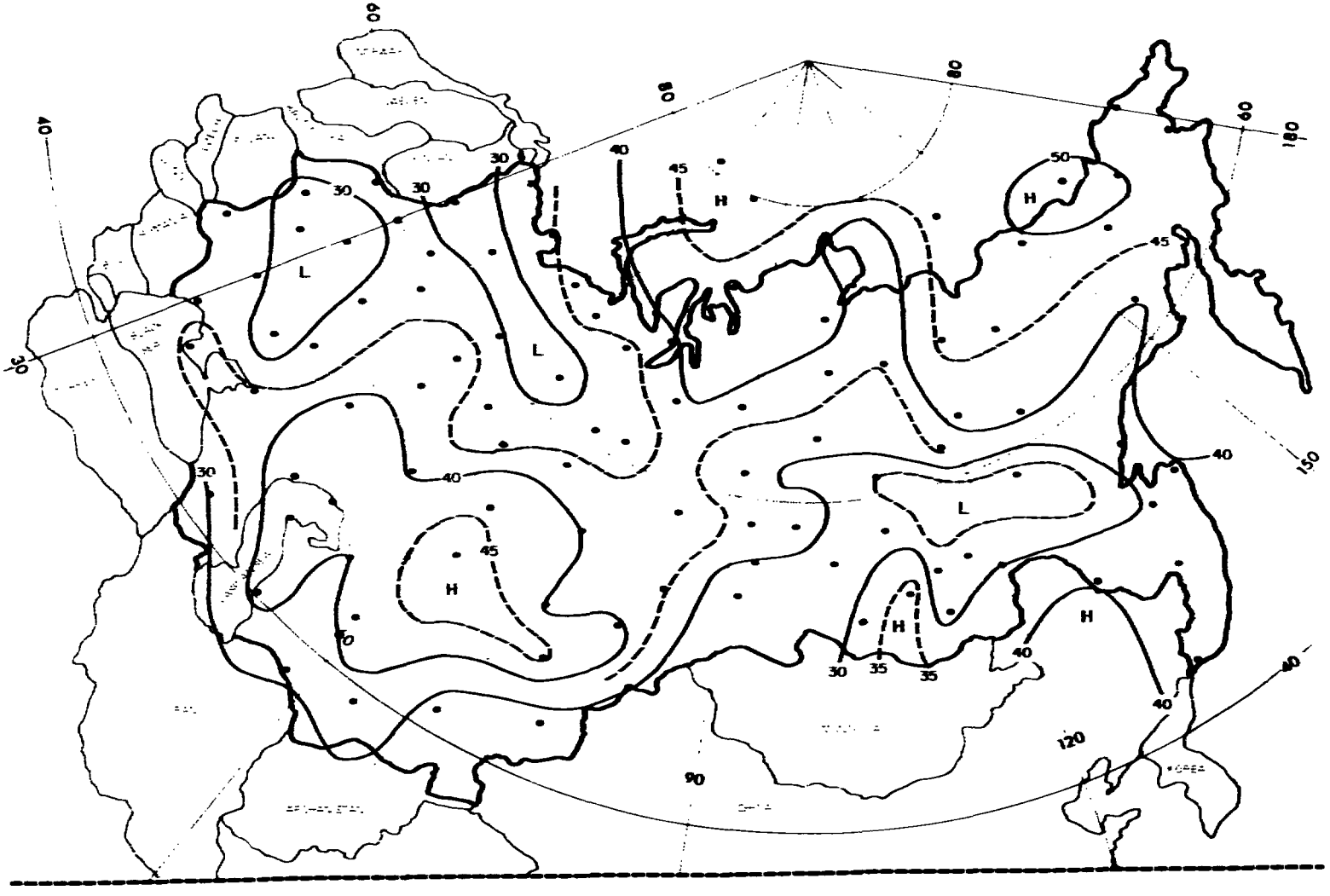

Figure 22. CFLOS Probabilities for Apr, 1200—1400 LST, 10° Elevation

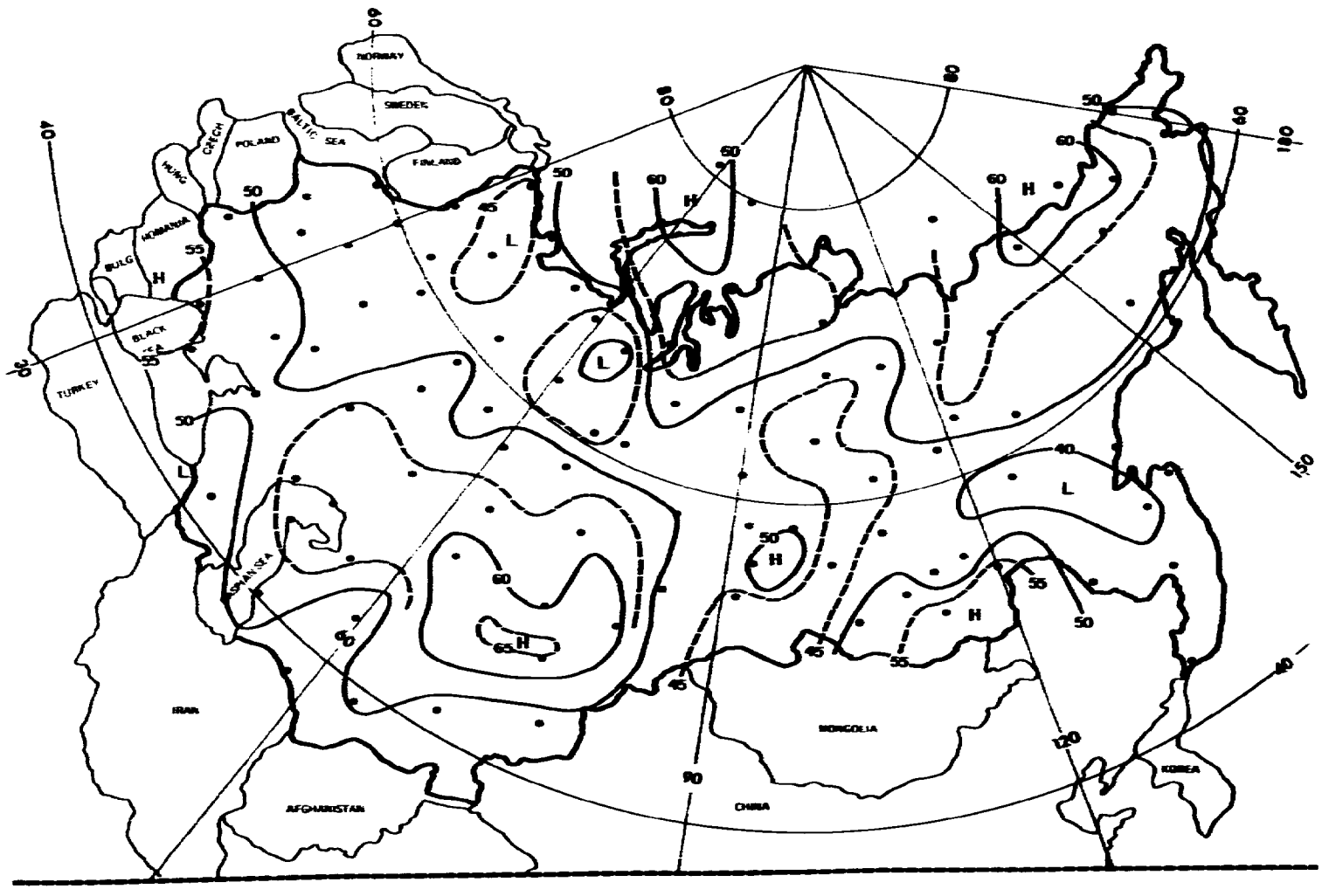

Figure 23. CFLOS Probabilities for Apr, 1800—2000 LST, 90° Elevation

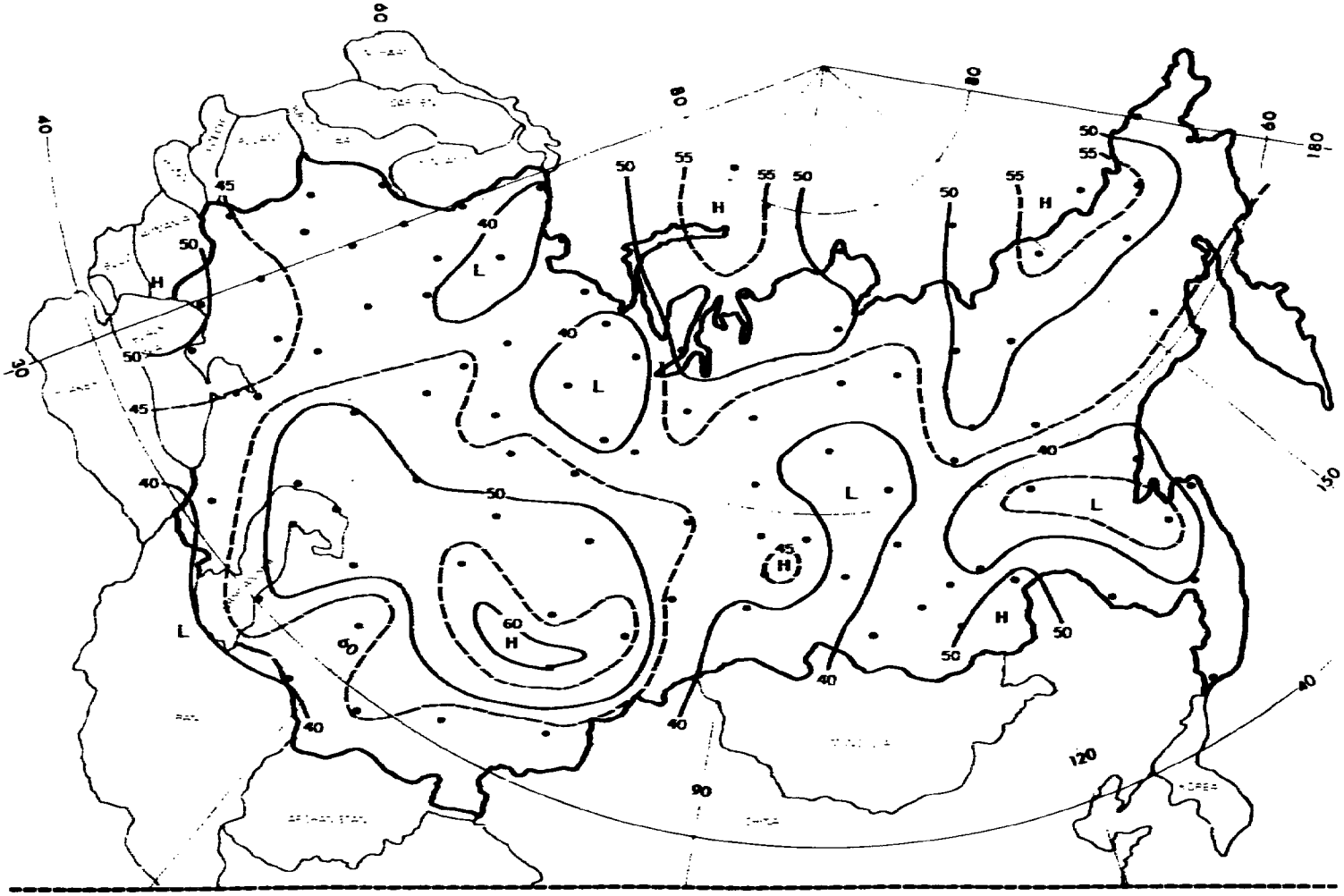

Figure 24. CFLOS Probabilities for Apr, 1800—2000 LST, 30° Elevation

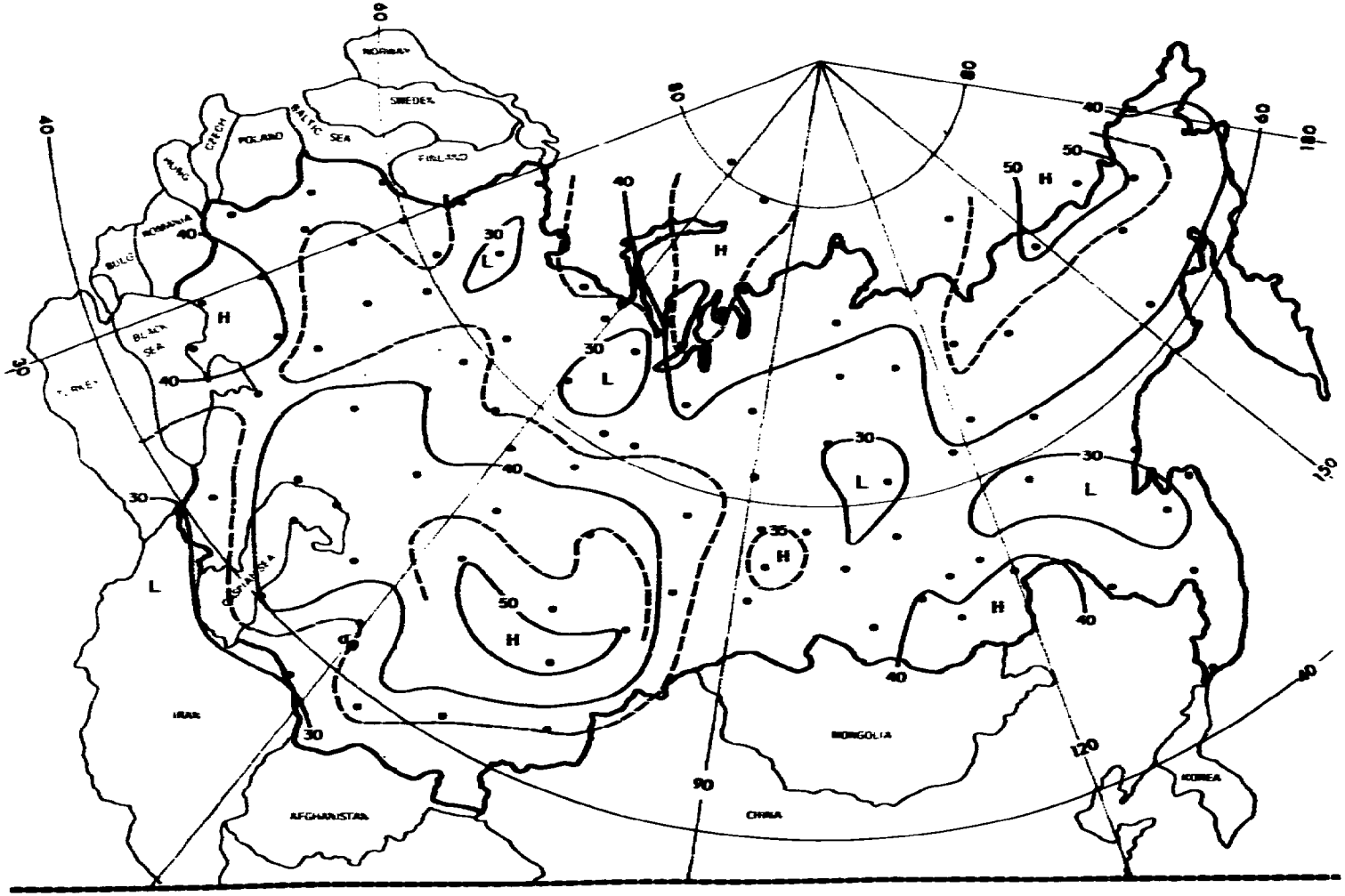

Figure 25. CFLOS Probabilities for Apr, 1800-2000 LST, 10° Elevation

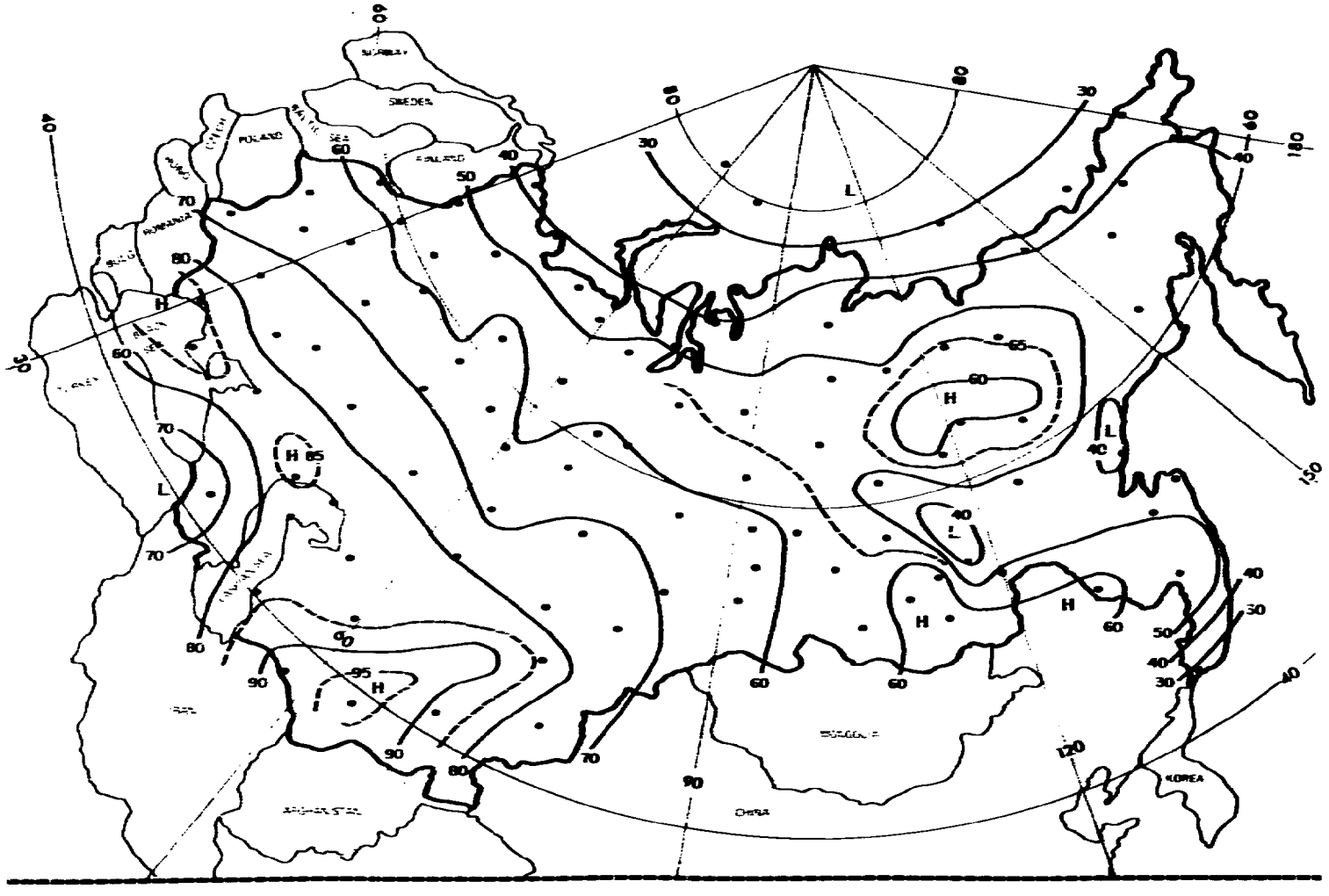

Figure 26. CFLOS Probabilities for July, 0000—0200 LST, 90° Elevation

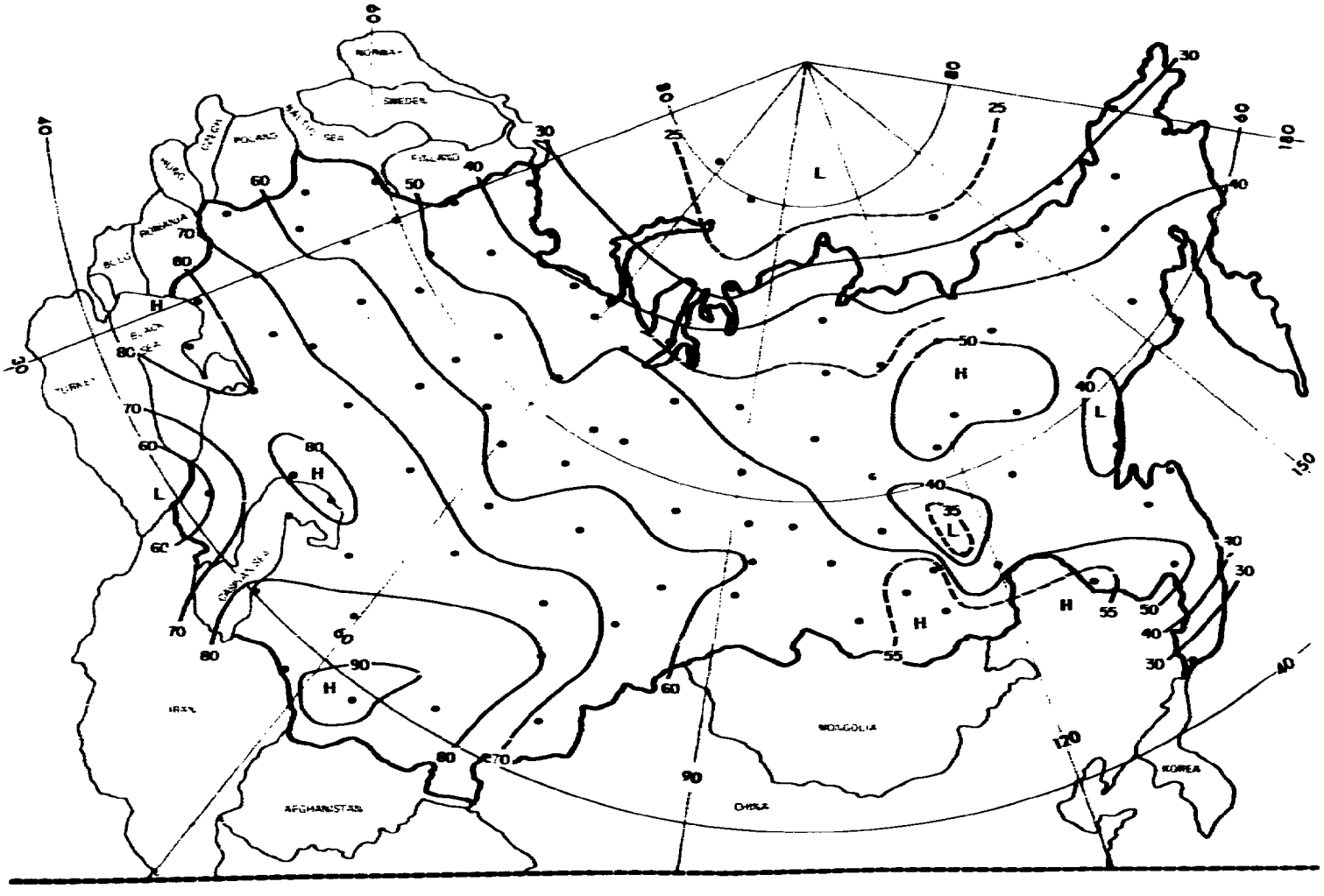

Figure 27. CFLOS Probabilities for July, 0000—0200 LST, 30° Elevation

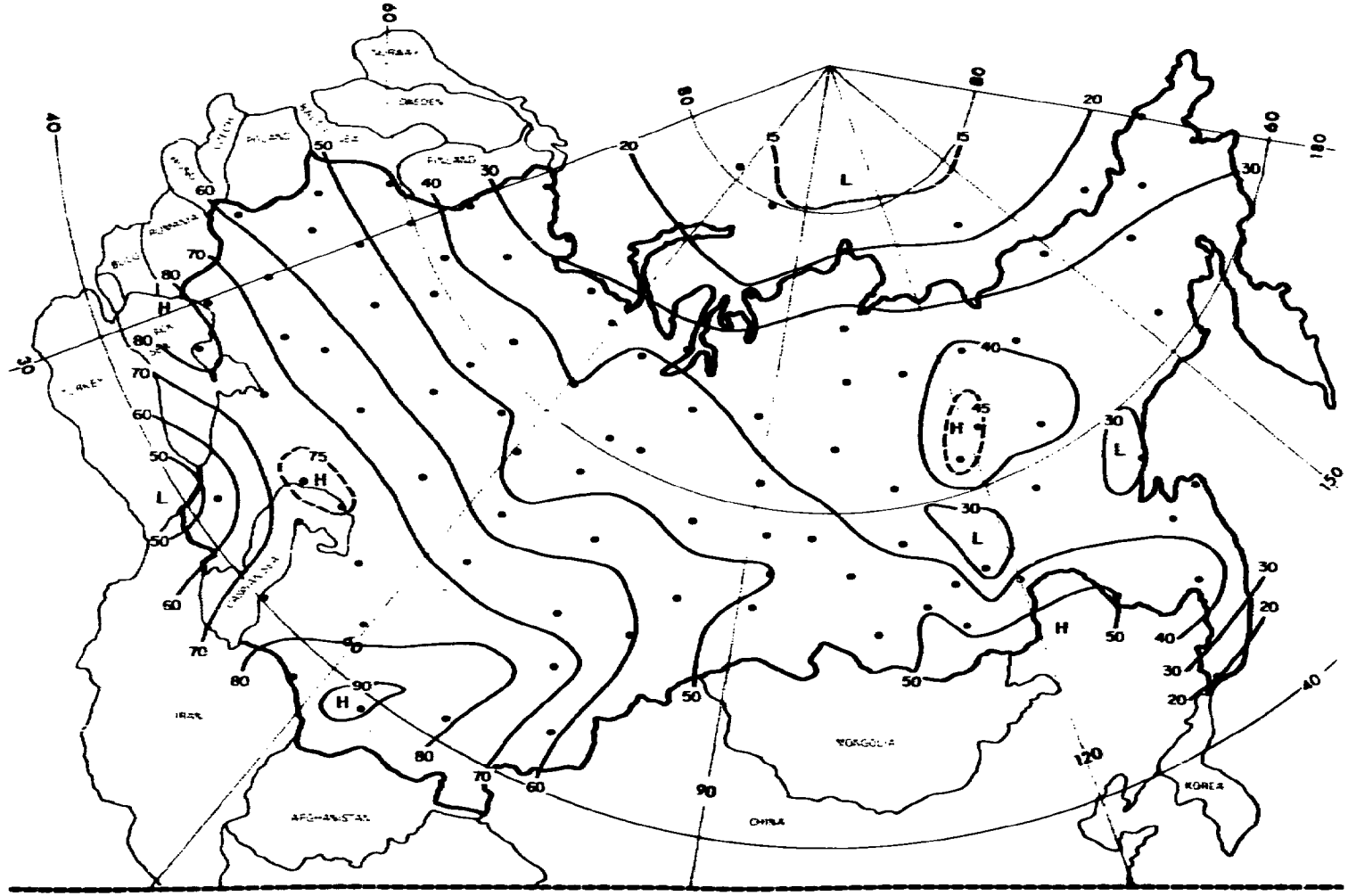

Figure 28. CFLOS Probabilities for July, 0000—0200 LST, 10° Elevation

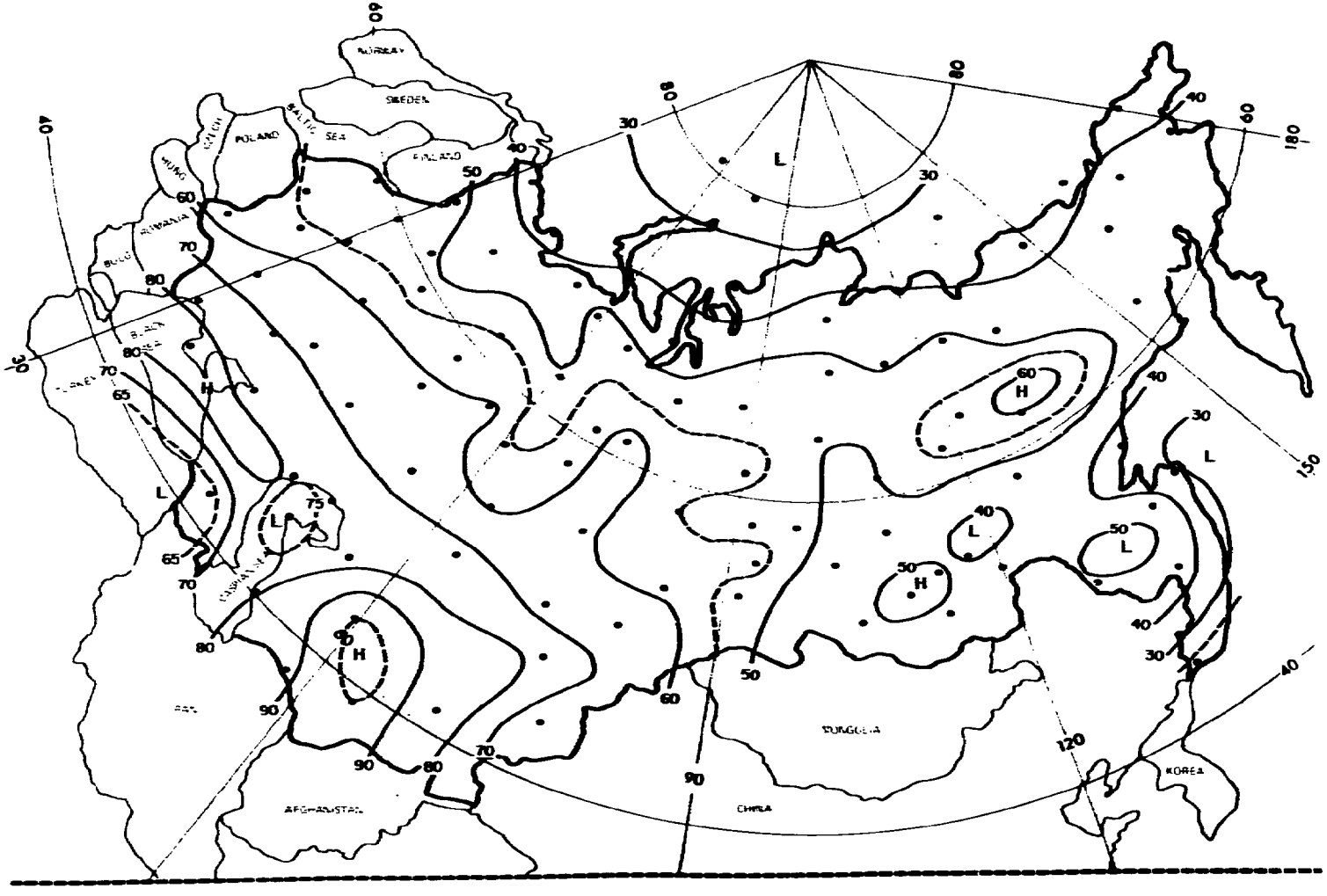

Figure 29. CFLOS Probabilities for July, 0600–0800 LST, 90° Elevation

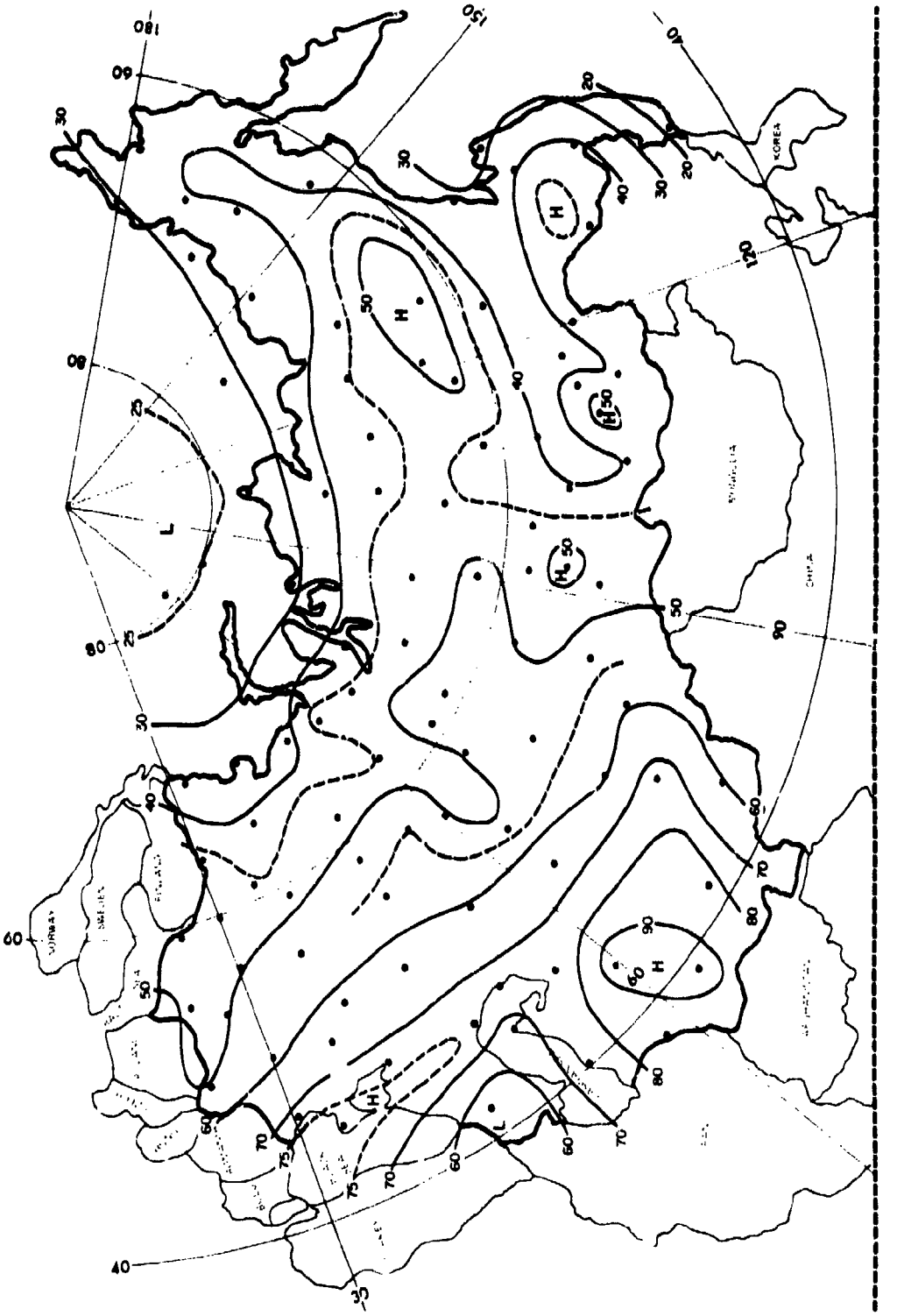

Figure 30. CFLOS Probabilities for July, 0600–0800 LST, 30° Elevation

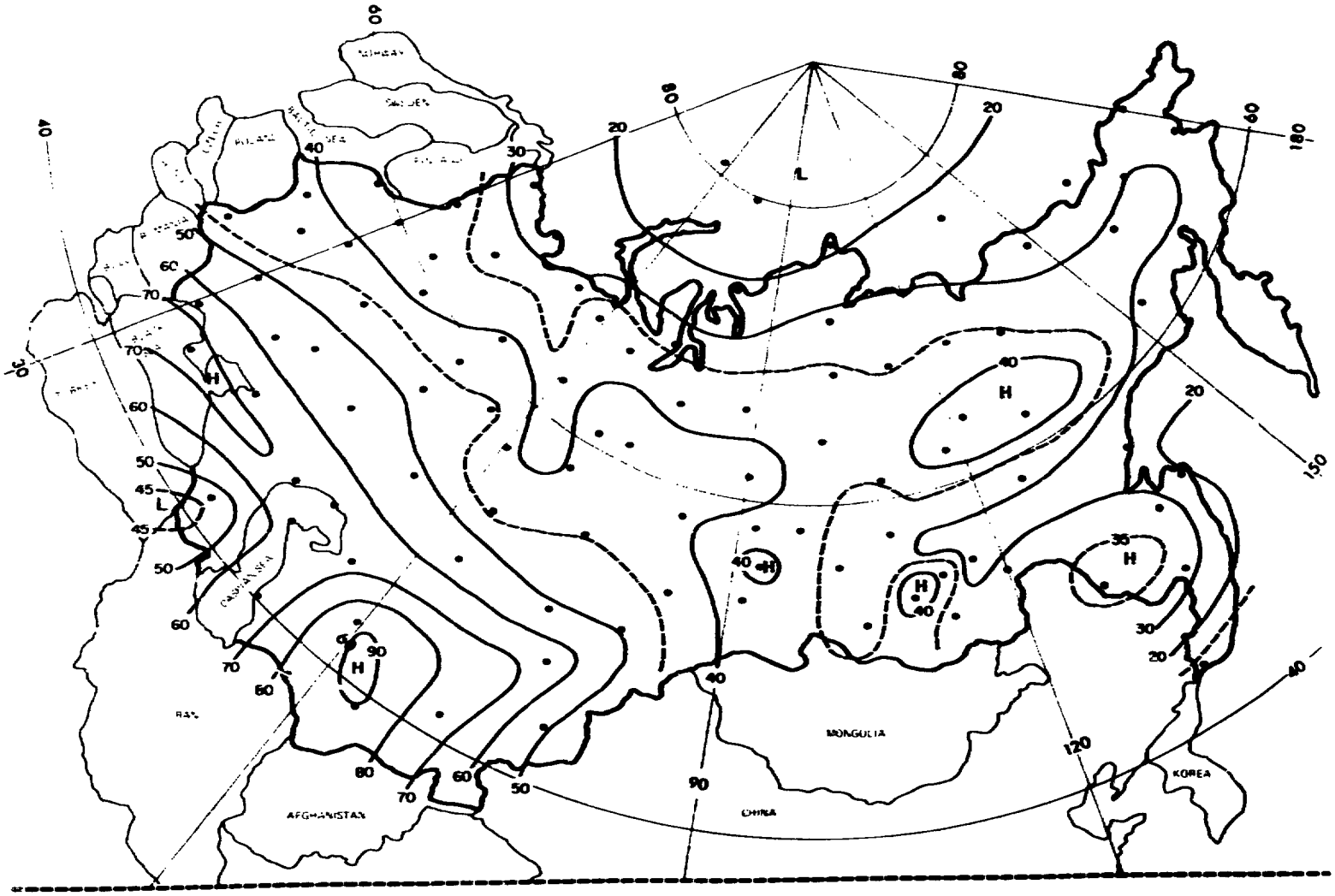

Figure 31. CFLOS Probabilities for July, 0600—0800 LST, 10° Elevation

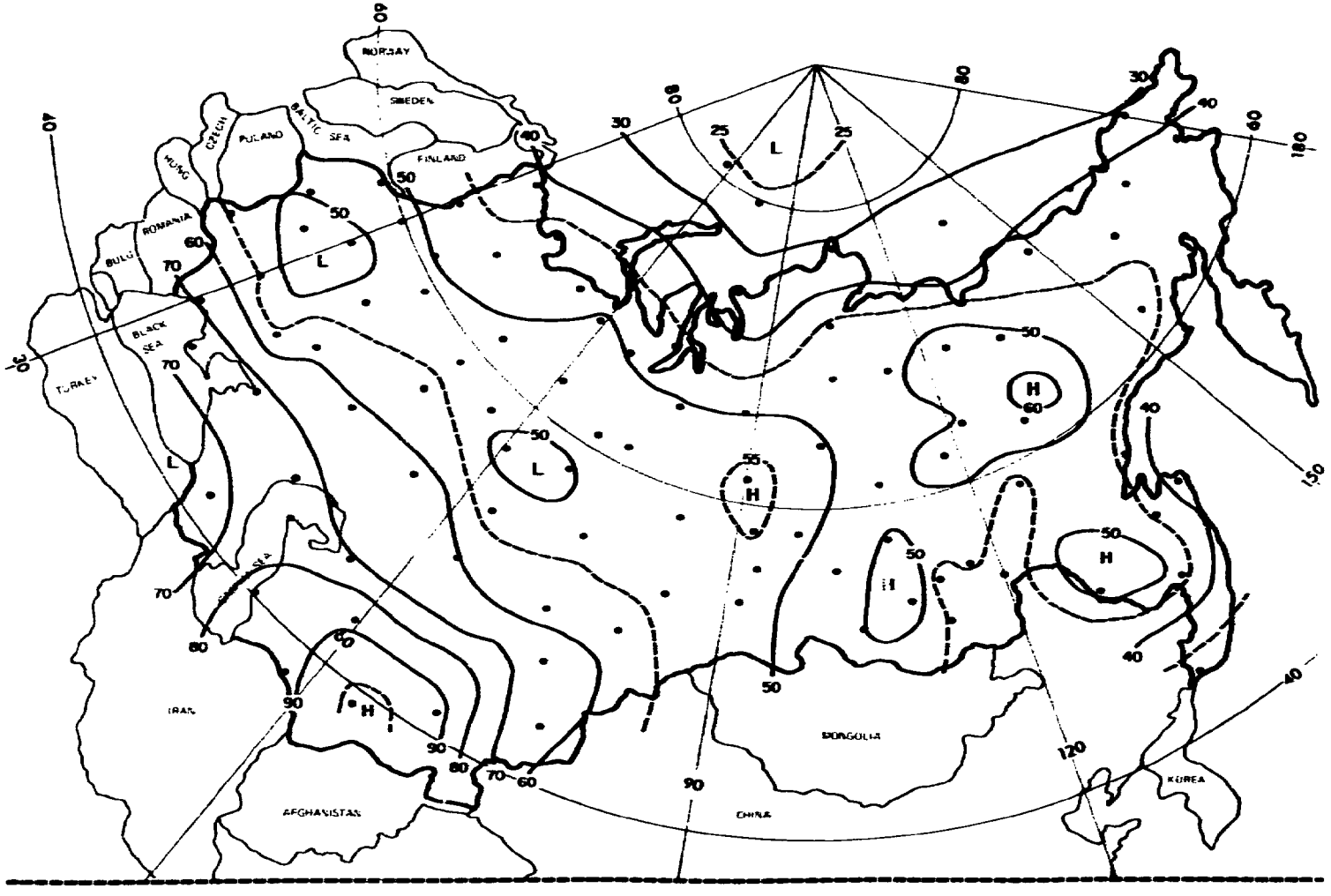

Figure 32. CFLOS Probabilities for July, 1200—1400 LST, 90° Elevation

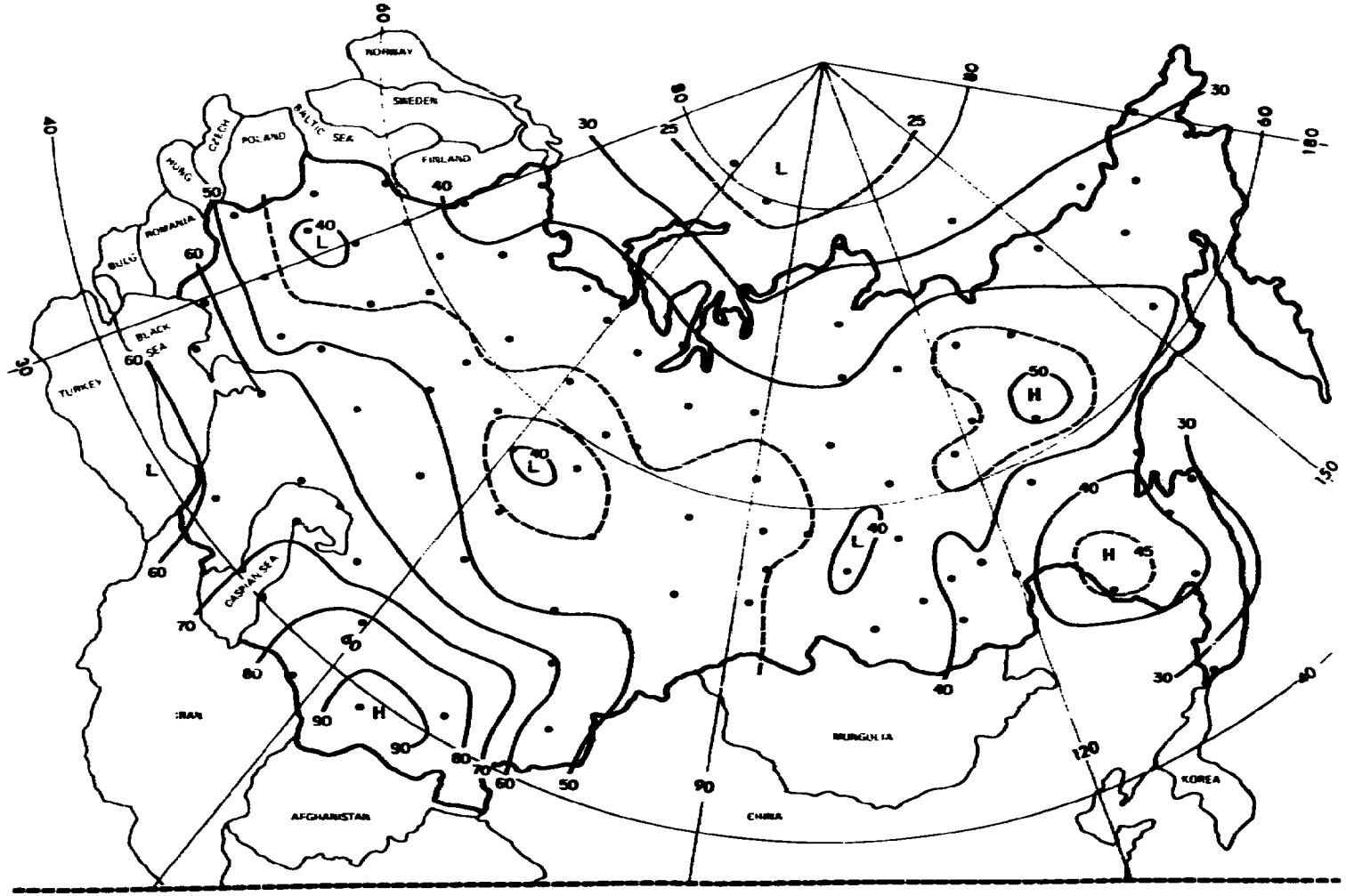

Figure 33. CFLOS Probabilities for July, 1200—1400 LST, 30° Elevation

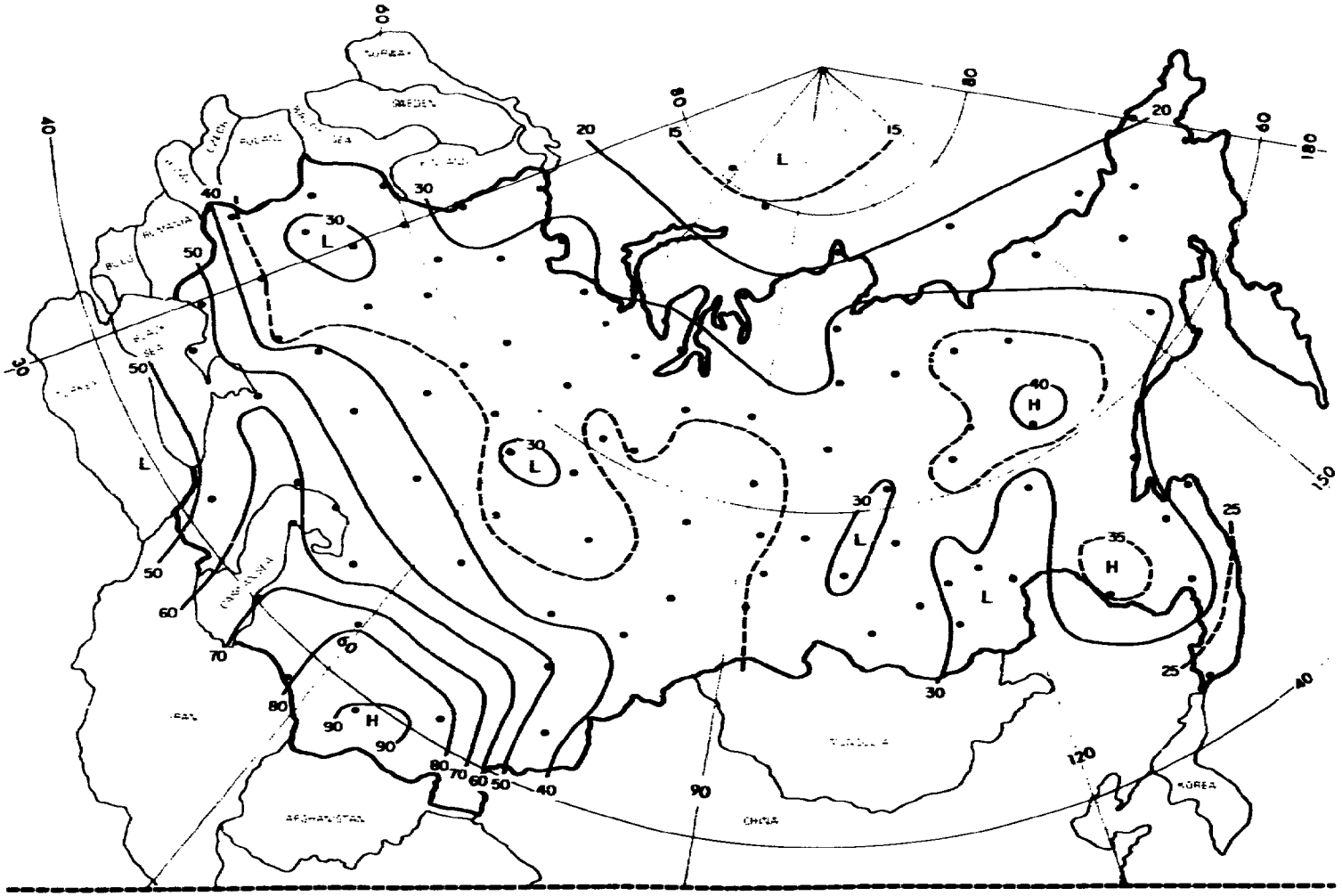

Figure 34. CFLOS Probabilities for July, 1200—1400 LST, 10° Elevation

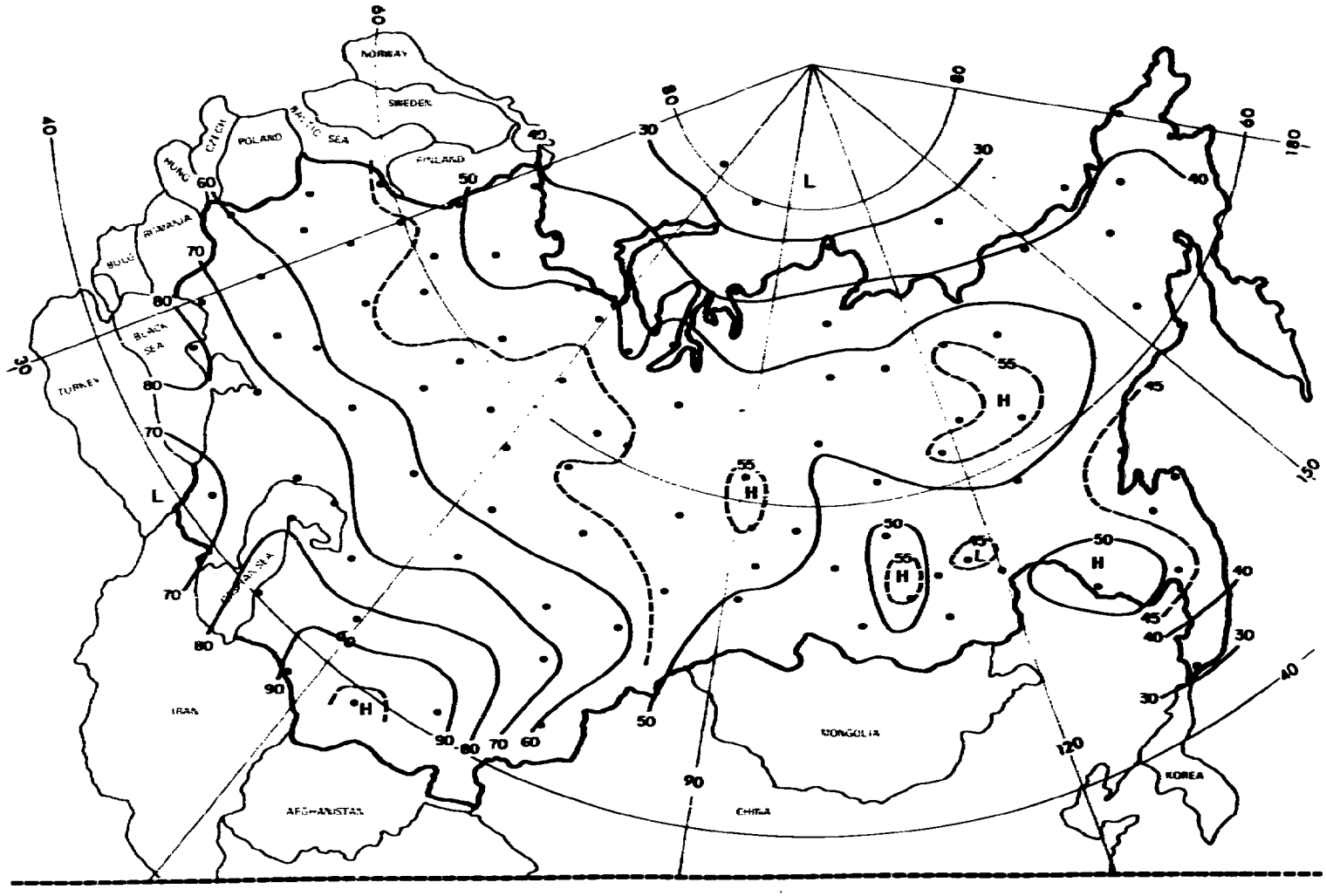

Figure 35. CFLOS Probabilities for July, 1800—2000 LST, 90° Elevation

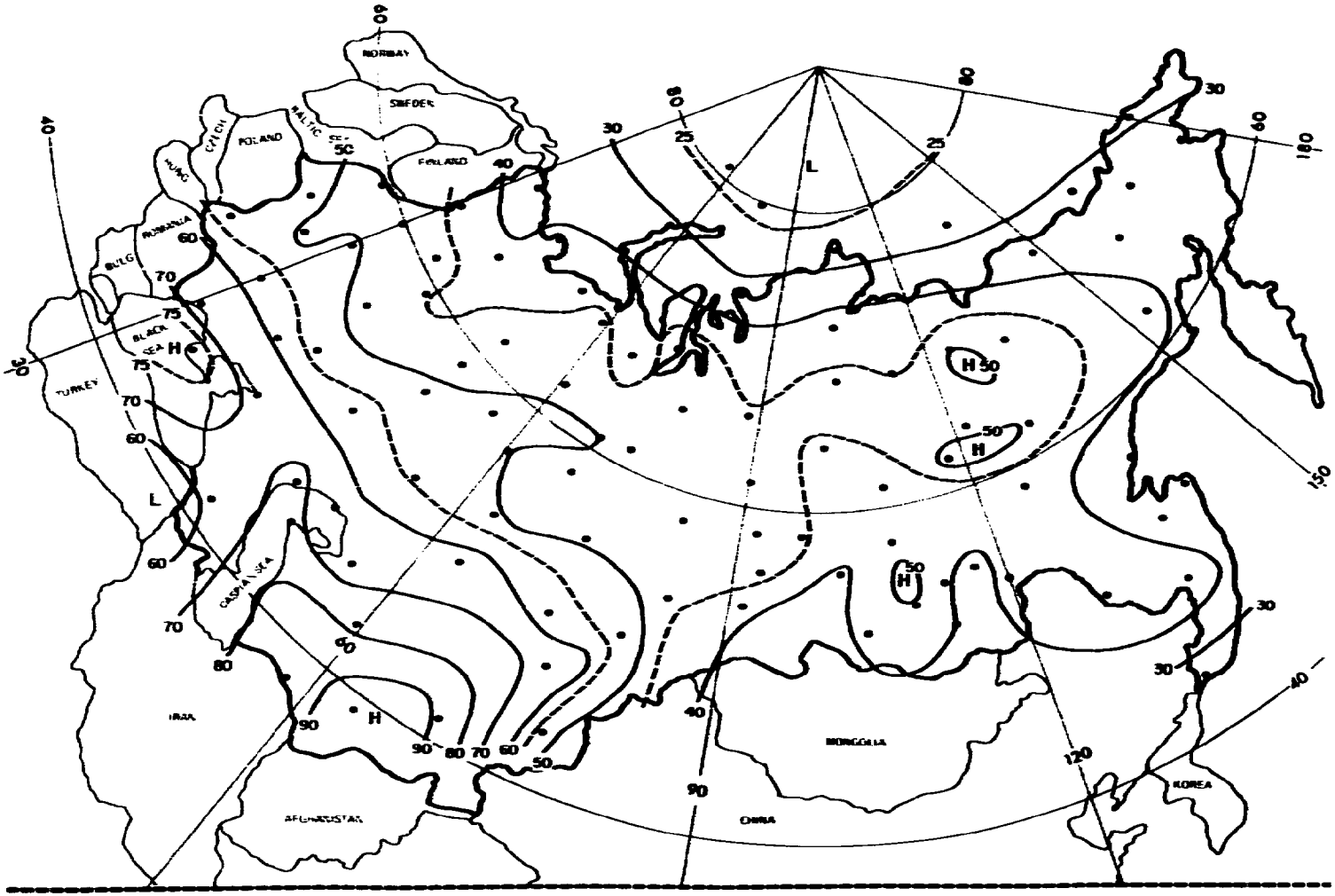

Figure 36. CFLOS Probabilities for July, 1800—2000 LST, 30° Elevation

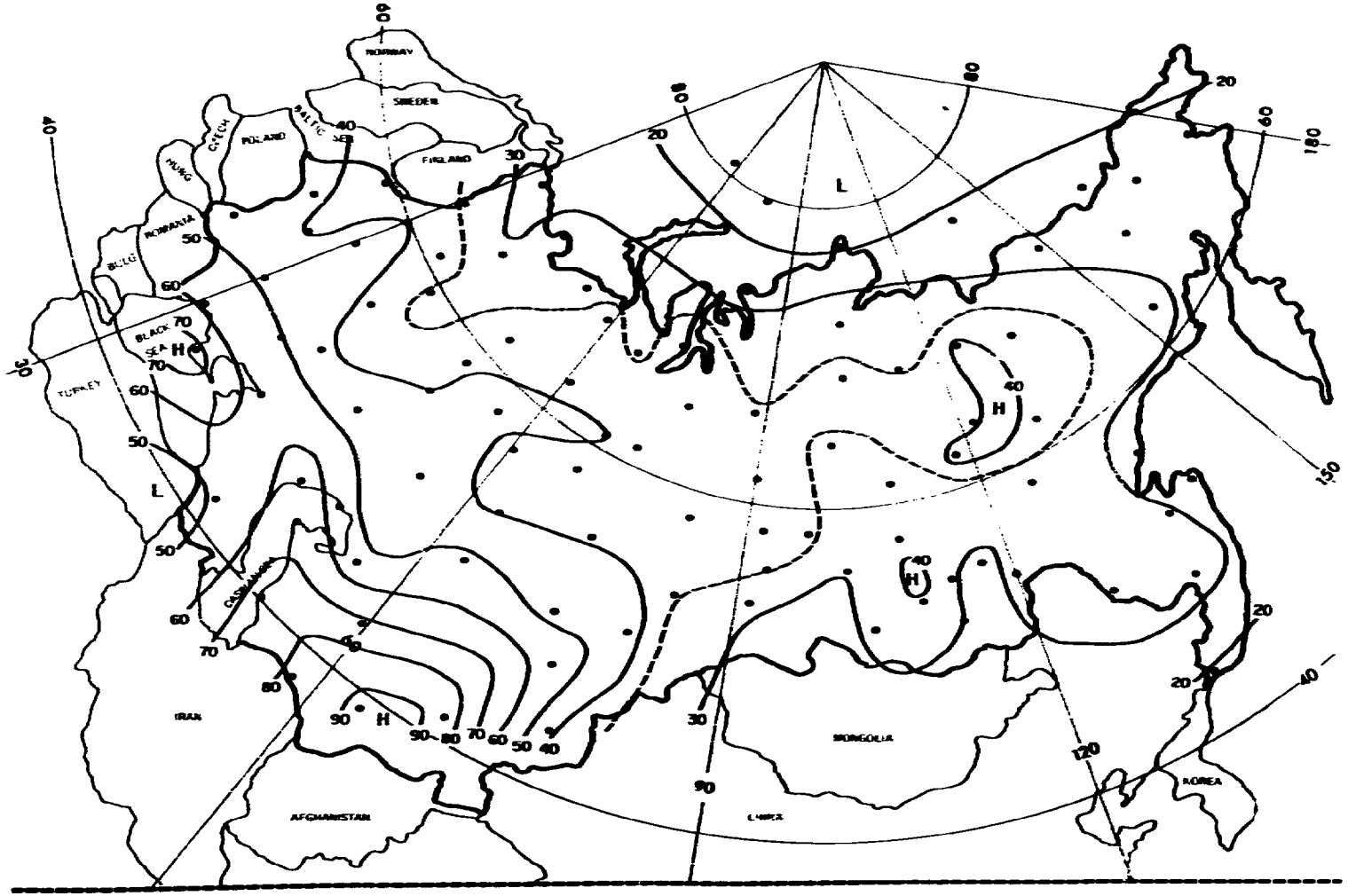

Figure 37. CFLOS Probabilities for July, 1800—2000 LST, 10° Elevation

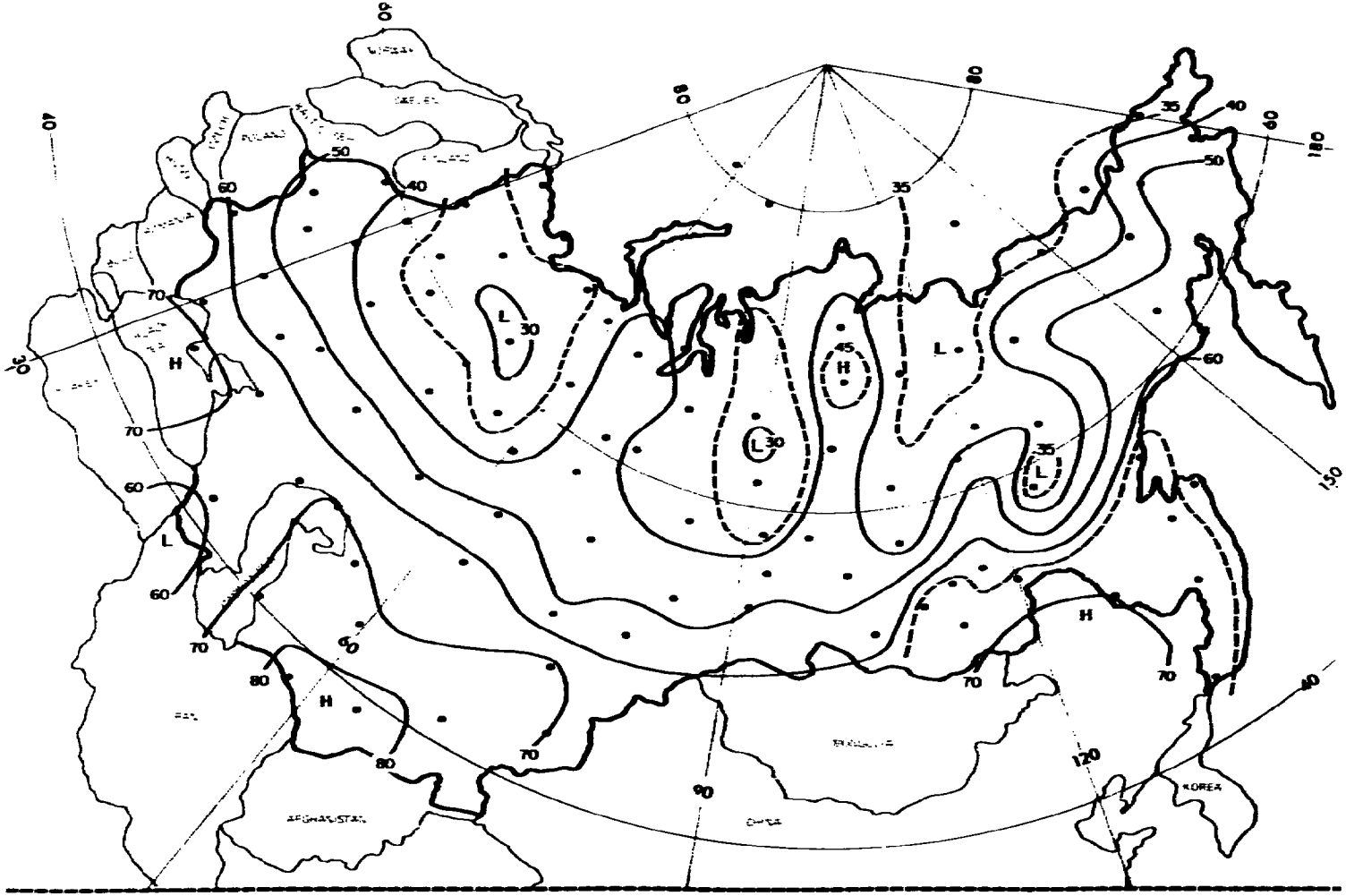

Figure 38. CFLOS Probabilities for Oct, 0000—0200 LST, 90° Elevation

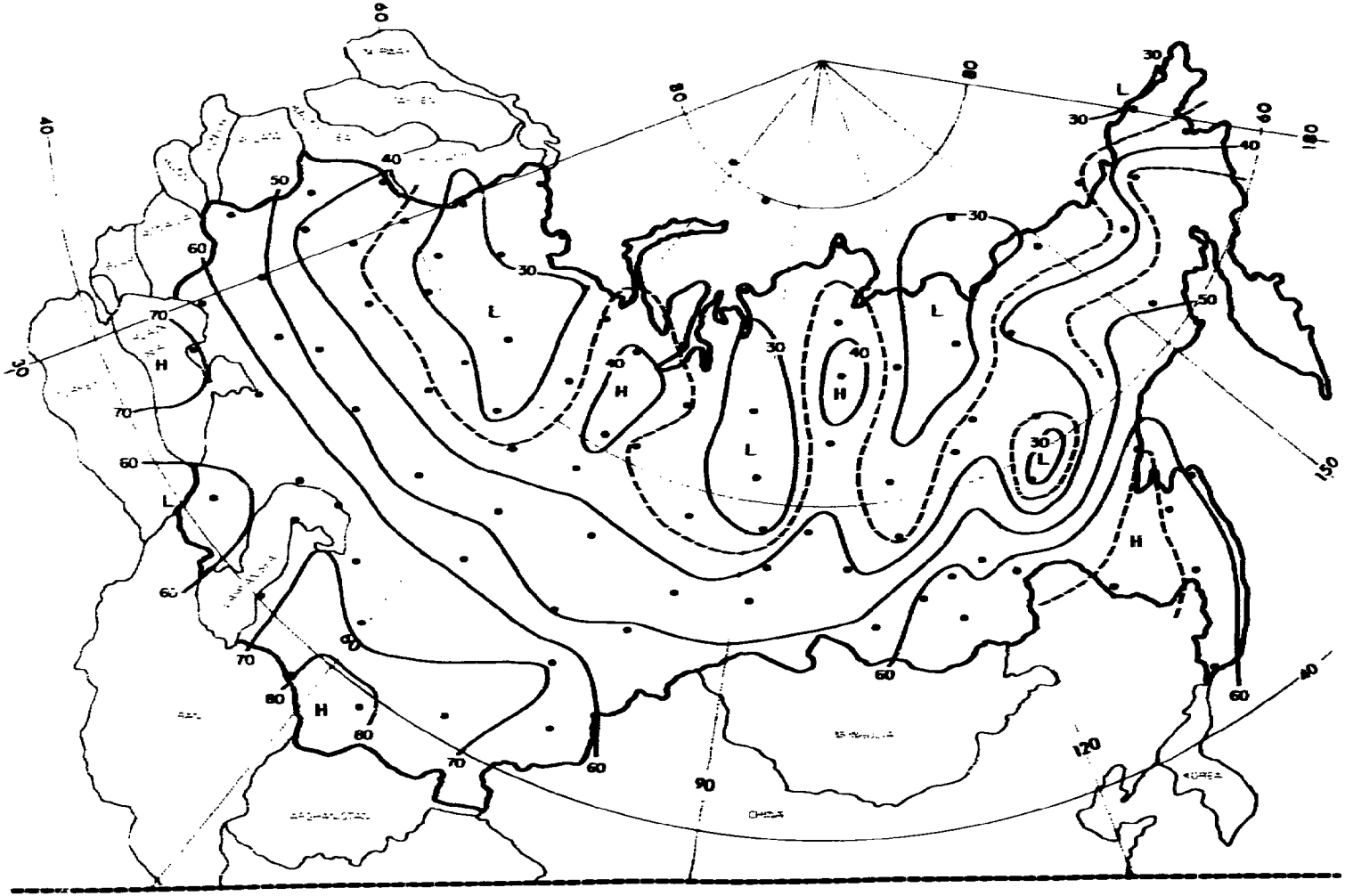

Figure 39. CFLOS Probabilities for Oct, 0000–0200 LST, 30° Elevation

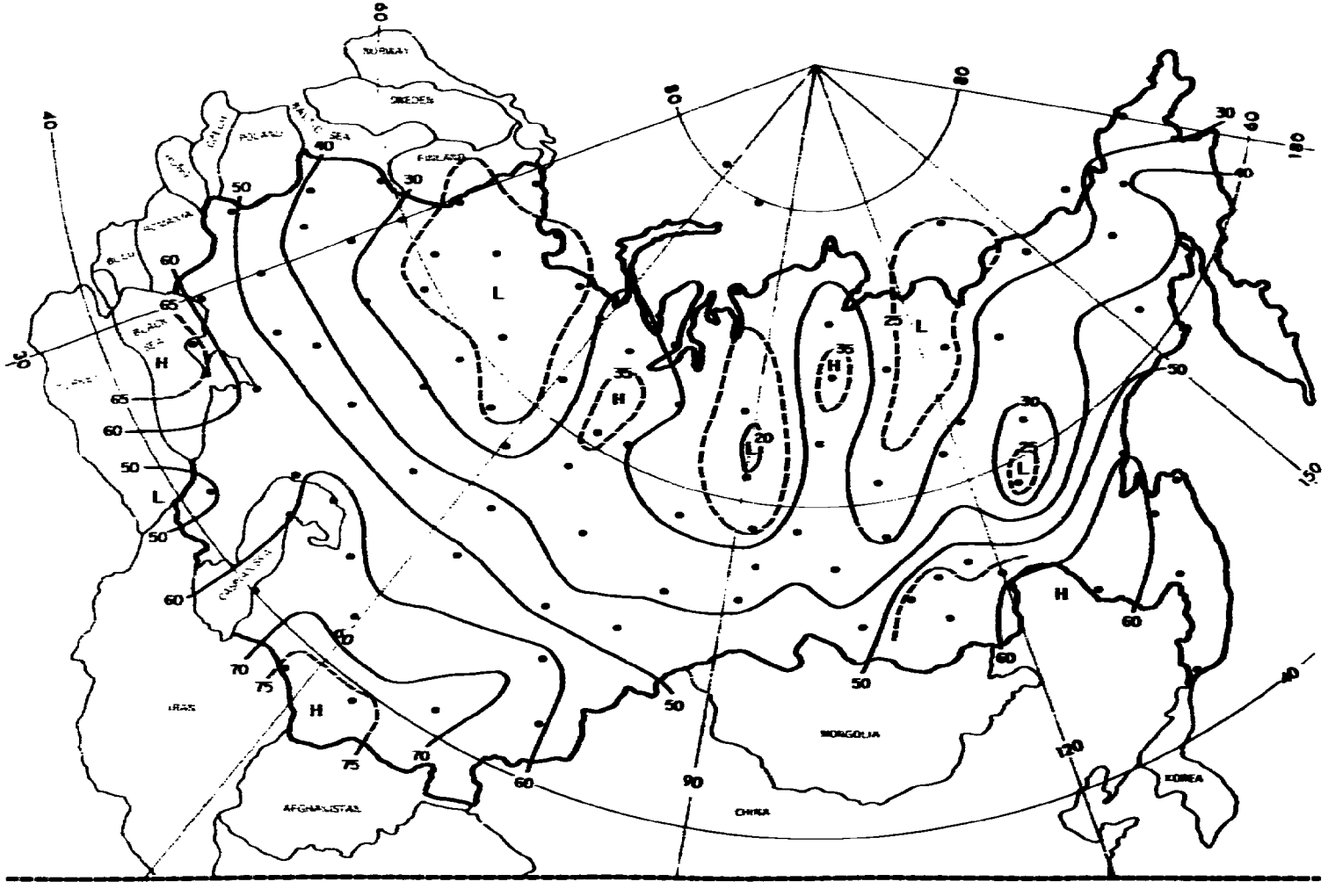

Figure 40. CFLOS Probabilities for Oct, 0000–0200 LST, 10° Elevation

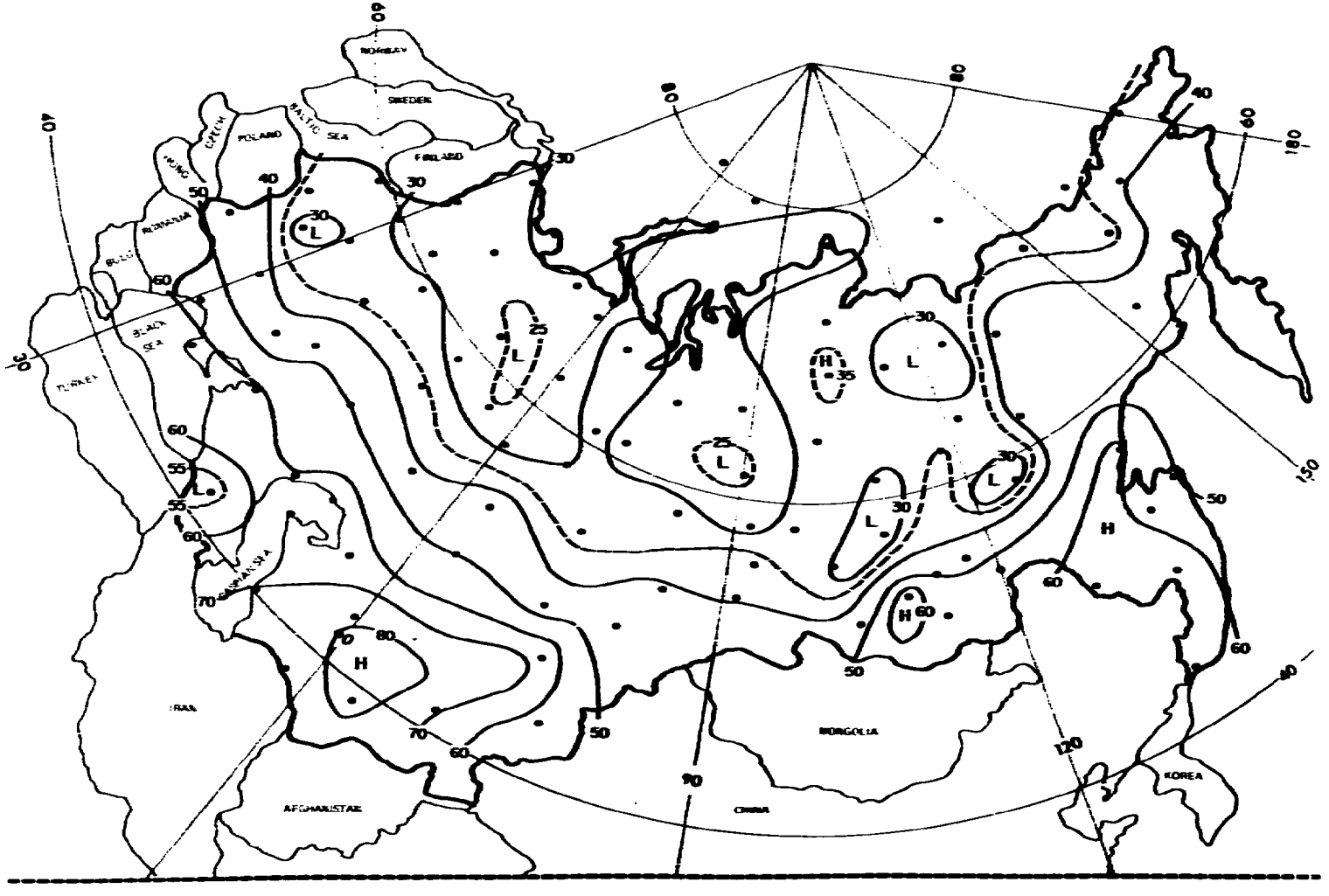

Figure 41. CFLOS Probabilities for Oct, 0600—0800 LST, 90° Elevation

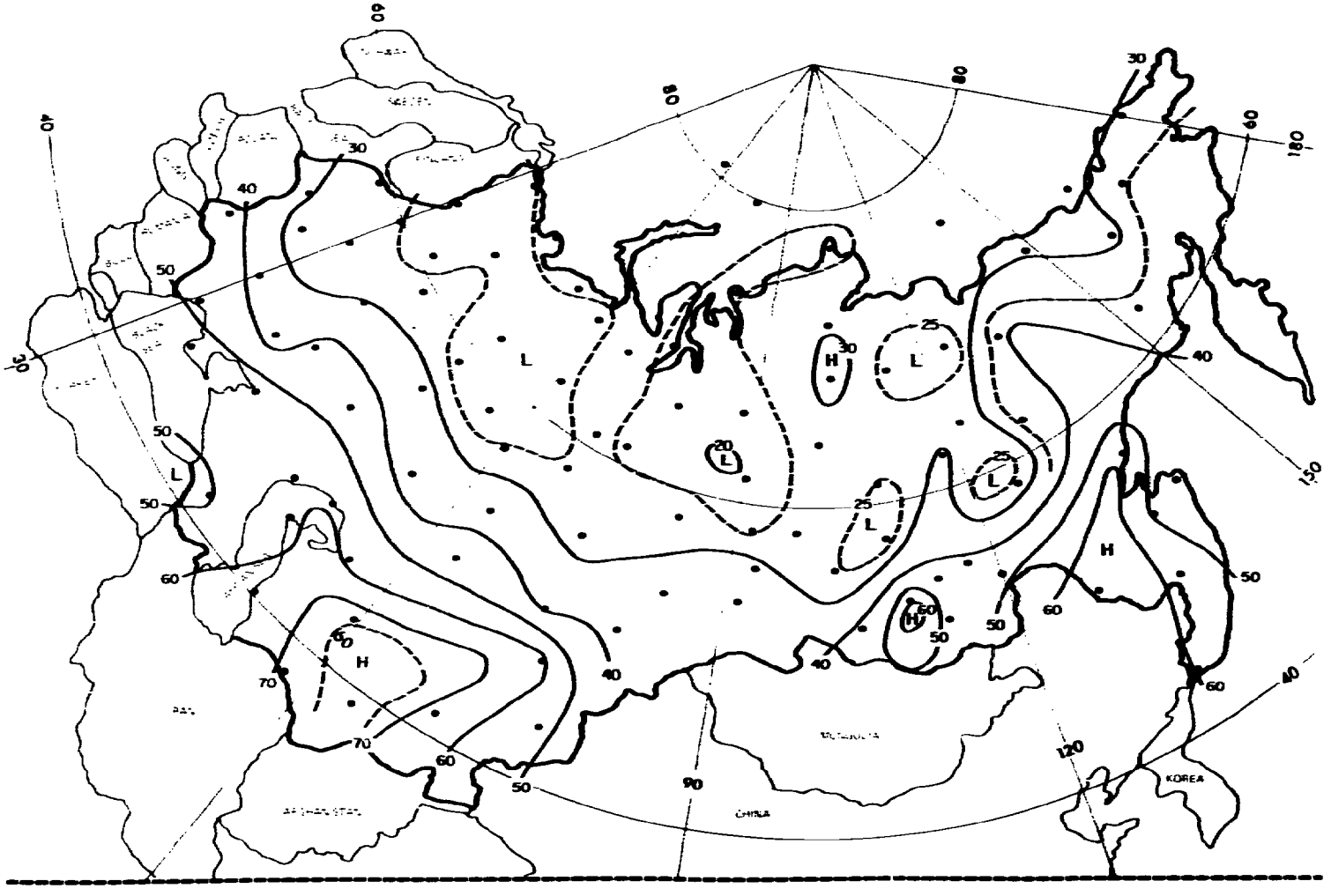

Figure 42. CFLOS Probabilities for Oct, 0600—0800 LST, 30° Elevation

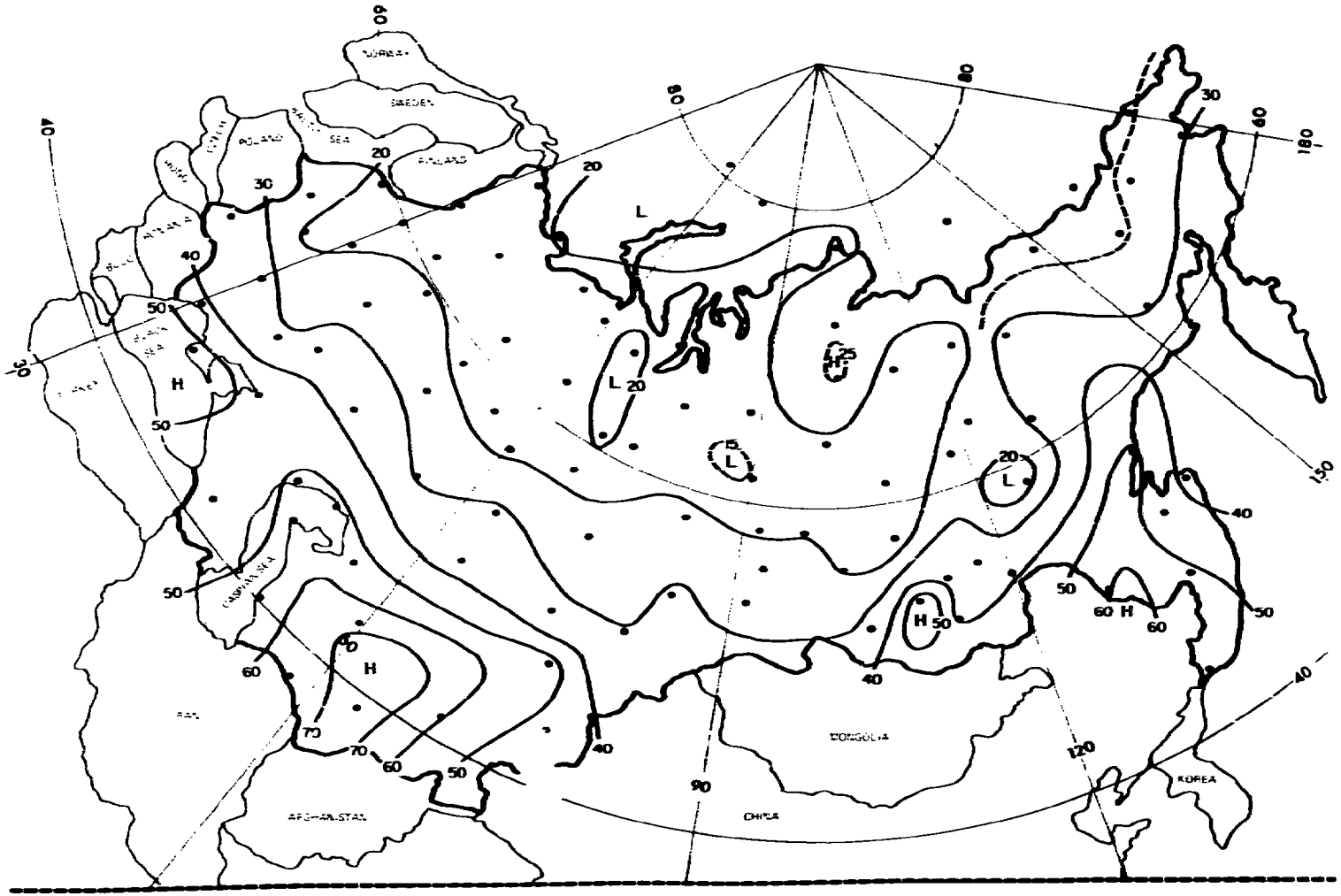

Figure 43. CFLOS Probabilities for Oct, 0600—0800 LST, 10° Elevation

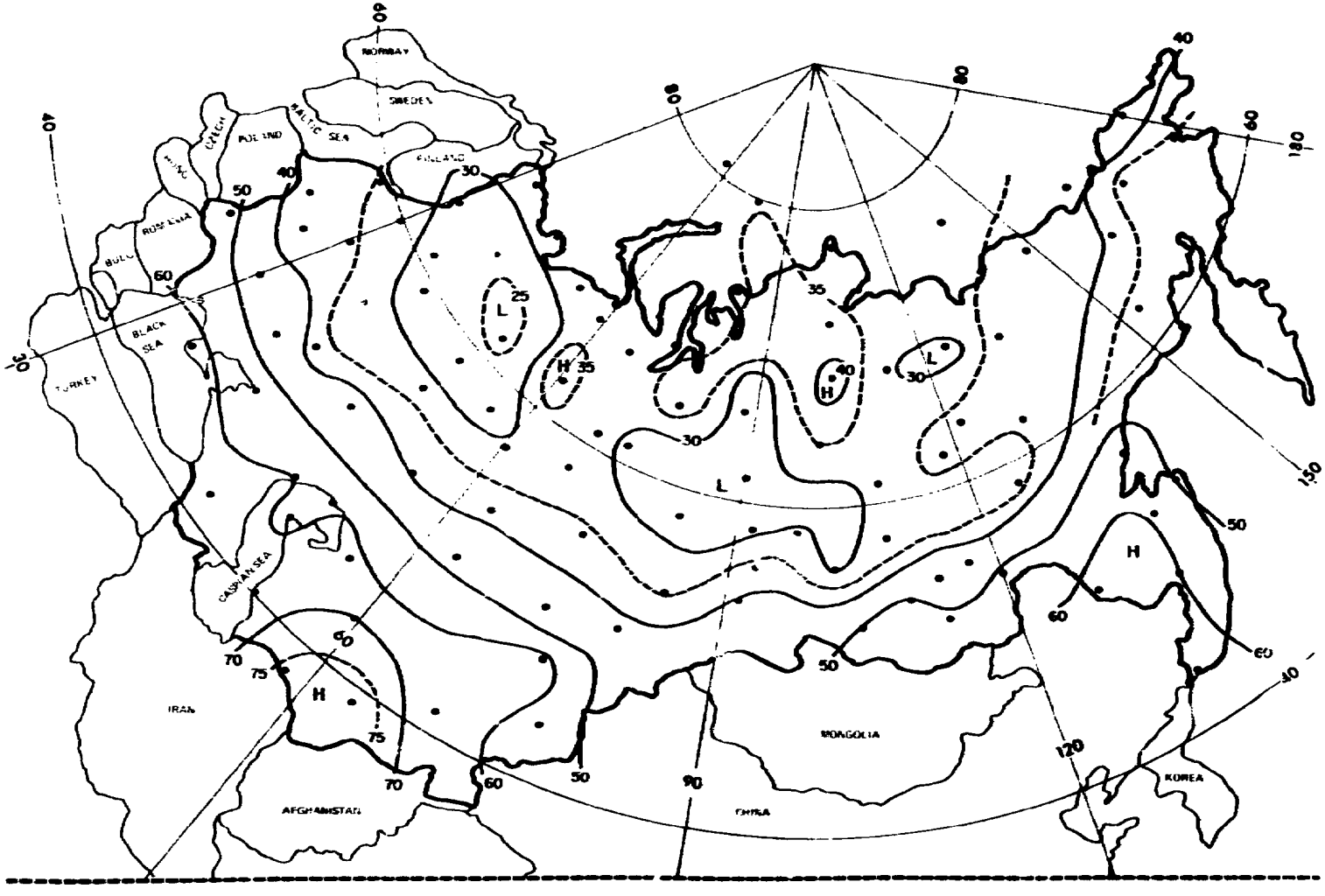

Figure 44. CFLOS Probabilities for Oct, 1200–1400 LST, 90° Elevation

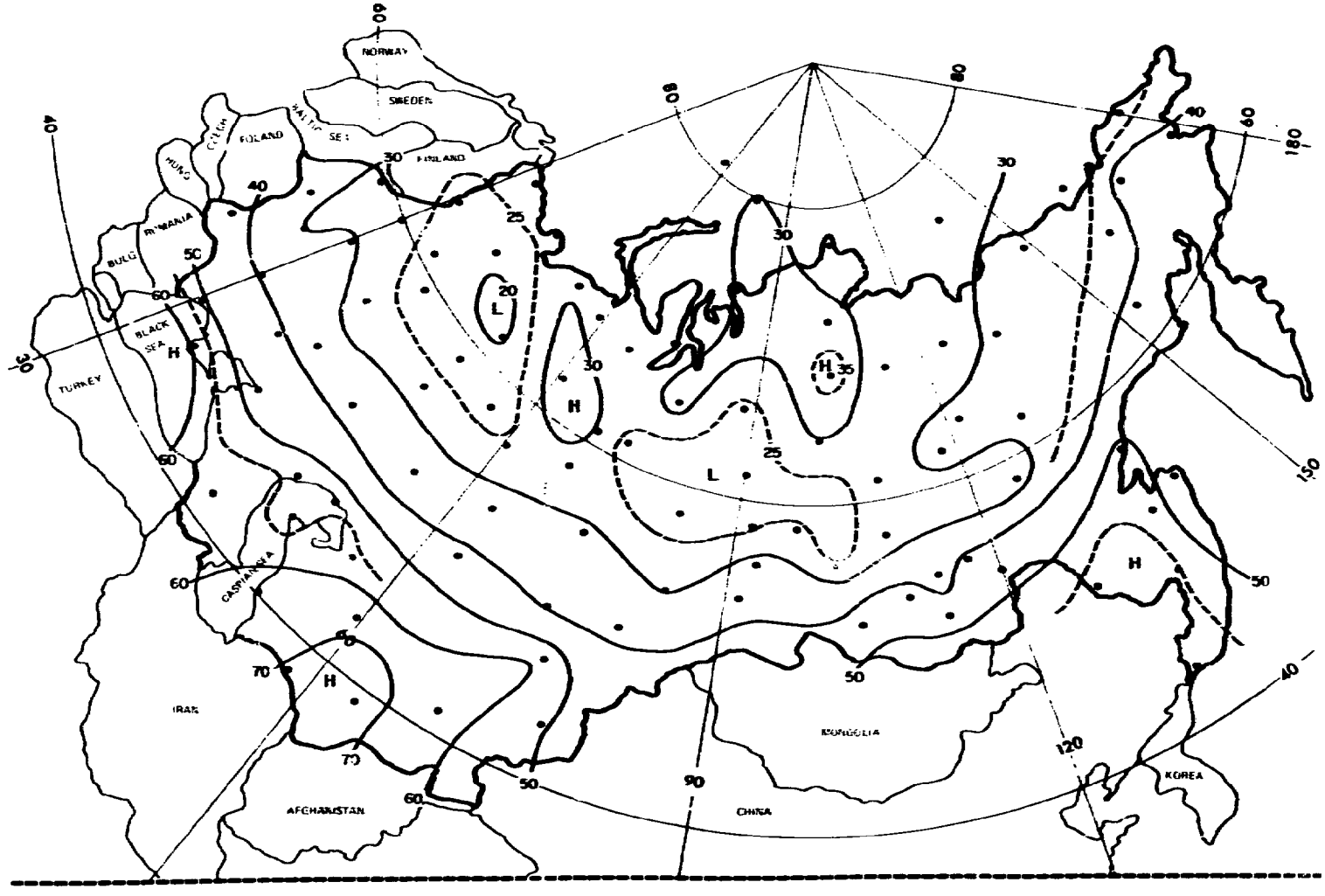

Figure 45. CFLOS Probabilities for Oct, 1200—1400 LST, 30° Elevation

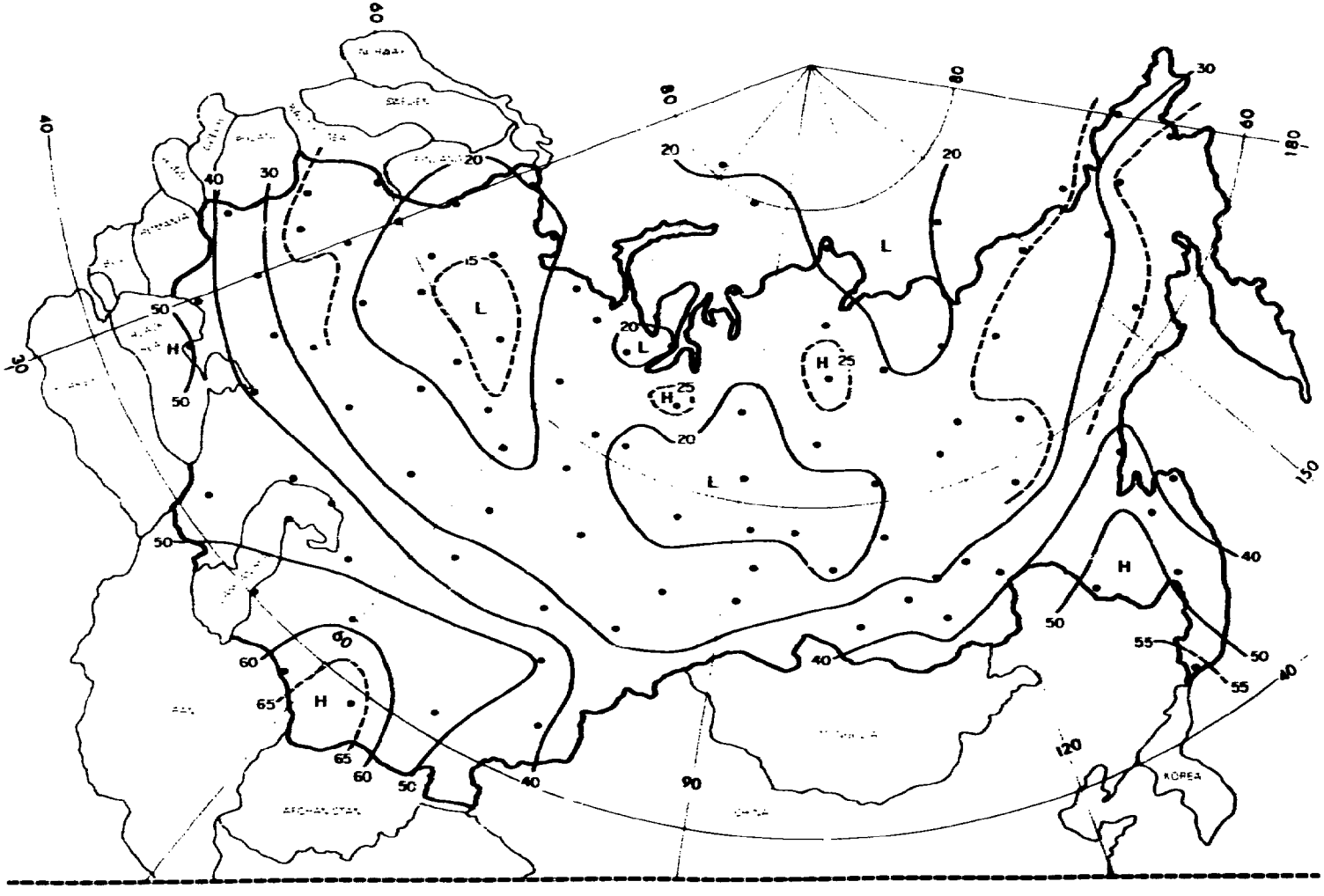

Figure 46. CFLOS Probabilities for Oct, 1200—1400 LST, 10° Elevation

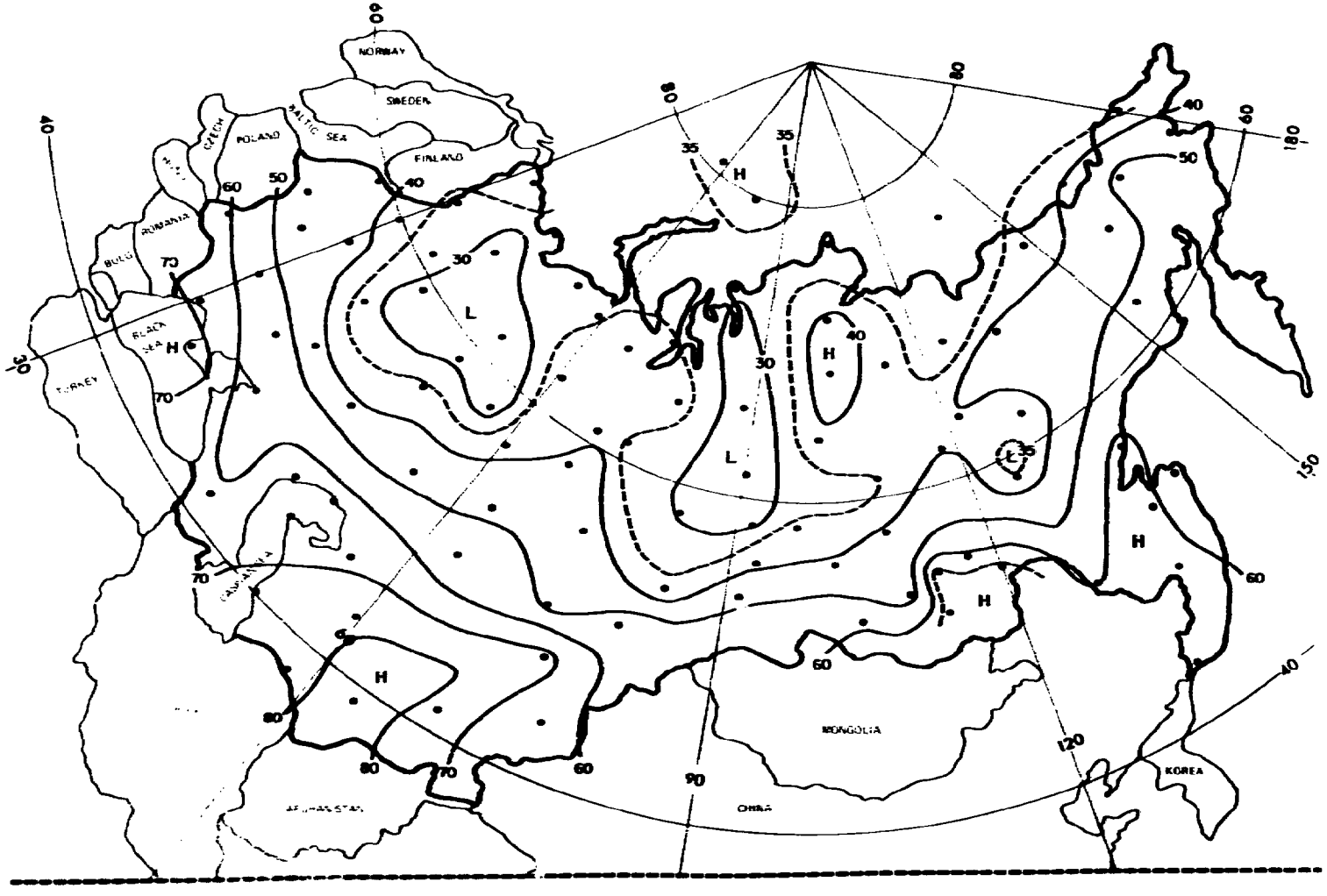

Figure 47. CFLOS Probabilities for Oct, 1800—2000 LST, 90° Elevation

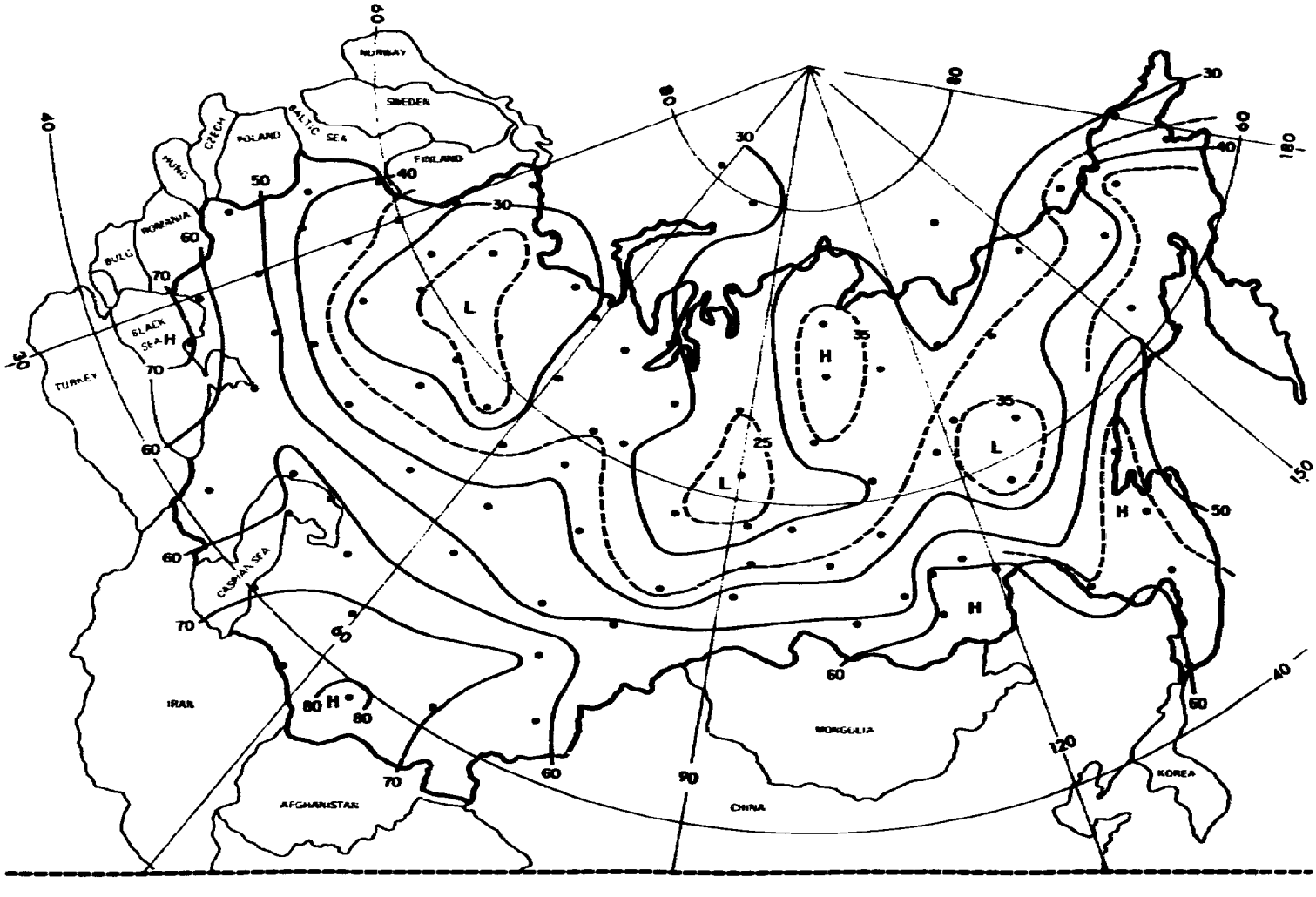

Figure 48. CFLOS Probabilities for Oct, 1800—2000 LST, 30° Elevation

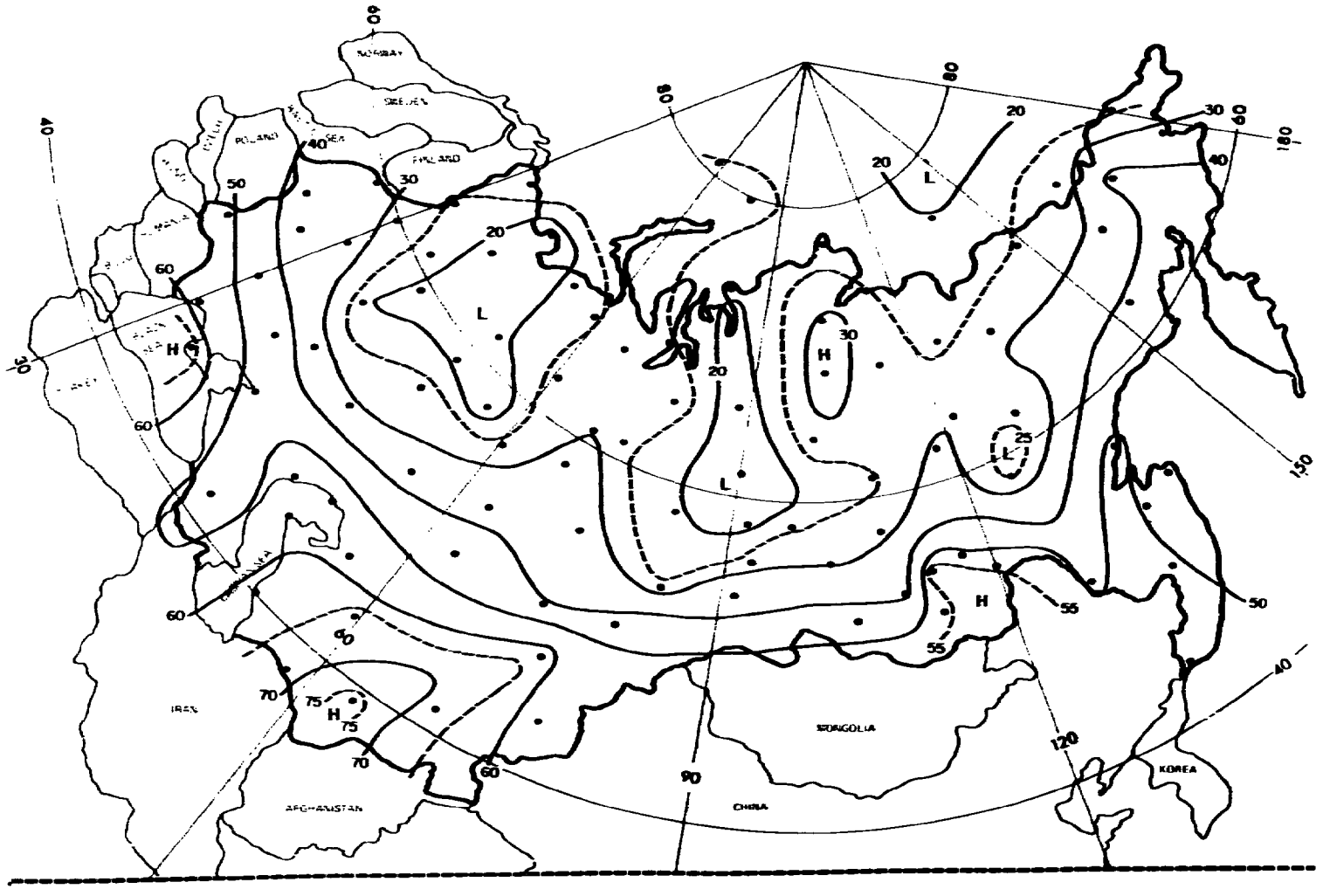

Figure 49. CFLOS Probabilities for Oct, 1800—2000 LST, 10° Elevation

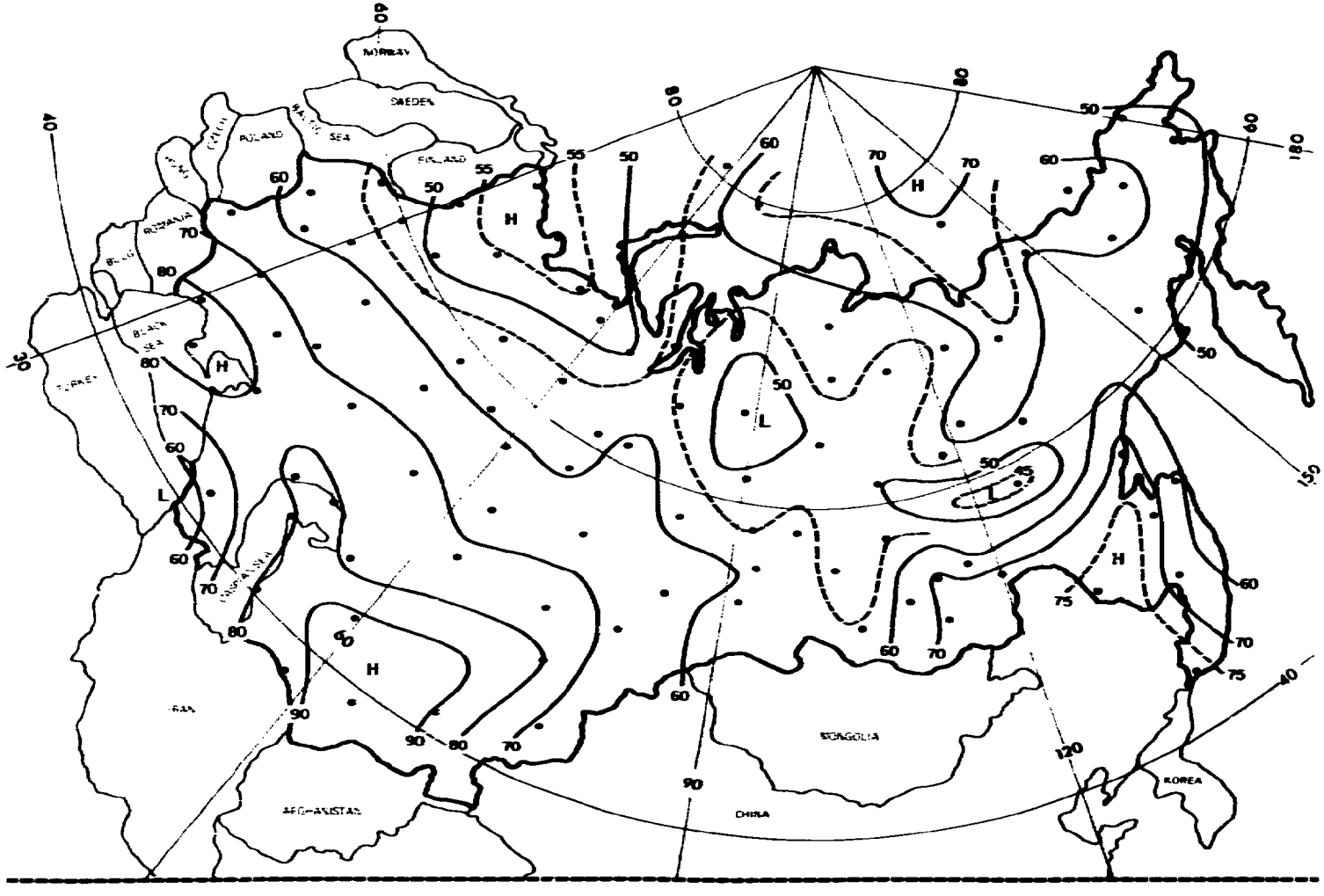

Figure 50. Highest CFLOS Probability, 30° Elevation

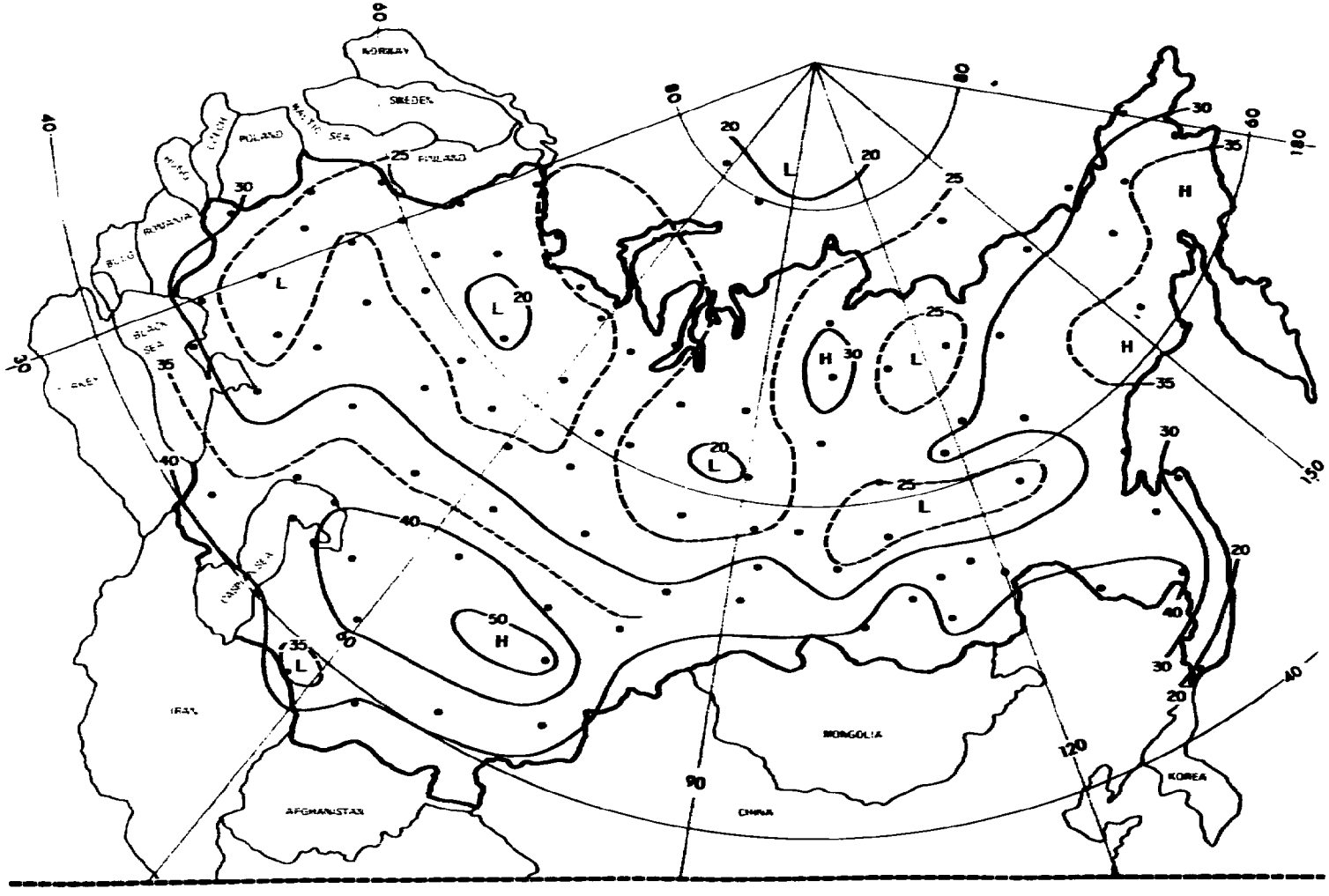

Figure 51. Lowest CFLOS Probability, 30° Elevation